

Simultaneous Inference for Empirical Best Predictors with a Poverty Study in Small Areas

Katarzyna Reluga*, María-José Lombardía† and Stefan Sperlich‡

Abstract

Today, generalized linear mixed models are broadly used in many fields. However, the development of tools for performing simultaneous inference has been largely neglected in this domain. A framework for joint inference is indispensable for comparisons of clusters or small areas. Therefore we introduce simultaneous confidence intervals and develop multiple testing procedures for empirical best predictors. We consider area- and unit-level models to study poverty rates in the counties of Galicia in Spain. In this context we illustrate to what extent existing methods fail. Simulation studies and complete asymptotic theory are also provided.

Key words: EBP, generalized mixed model, mixed parameter, small area estimation

*Katarzyna Reluga is PhD candidate and a teaching assistant at the University of Geneva, GSEM, RCS, Switzerland. E-mail: katarzyna.reluga@unige.ch.

†María-José Lombardía is Professor at the University of A Coruña, CITIC, Spain. E-mail: maria.jose.lombardia@udc.es.

‡Stefan Sperlich is Professor at the University of Geneva, GSEM, RCS, Switzerland. E-mail: stefan.sperlich@unige.ch.

The authors gratefully acknowledge support from the MINECO grants MTM2017-82724-R and MTM2014-52876-R, the Xunta de Galicia (Grupos de Referencia Competitiva ED431C-2016-015 and Centro Singular de Investigación de Galicia ED431G/01), all of them through the ERDF.

1 Introduction

It is commonly accepted that generalized linear mixed models (GLMMs) are particularly suitable for modeling clustered and correlated data with categorical or count outcomes, see Jiang (2007) or Demidenko (2013) for a comprehensive overview. They have become ubiquitous in applied statistics wherever a natural clustering arises, for example in biometrics, environmetrics, medicine, psychology or in small area estimation (SAE). In the latter, GLMMs serve to analyze surveys on a disaggregated level such as local poverty or unemployment rates. Despite a steadily increasing interest (e.g., in SAE to guide resource allocation or predict sustainable development goal indicators), the development of methods for simultaneous inference about the resulting predictors for a mixed parameter is missing. This is surprising as only those methods make joint considerations of clusters statistically valid. For example, essentially all available $(1 - \alpha)$ -confidence intervals (CIs) for mixed parameter (except the credibility intervals of Ganesh (2009)) are constructed such that for each survey study at least $\alpha 100\%$ of the CIs do not contain the true value – no matter whether first- or second-order corrected CIs are considered. Undoubtedly, practitioners do compare, but so far without valid statistical tools. It is worth mentioning that we aim to close this distressing gap, not to improve already existing methods.

Specifically, we introduce simultaneous confidence intervals (SCIs) and multiple test procedures (MTPs) for the empirical best predictor (EBP) of Jiang (2003). Hobza and Morales (2016) implemented the EBP for unit-level GLMM and Boubeta et al. (2016) for area-level GLMM; both in order to study poverty in small areas. Our tools are designed for any GLMM within the exponential family, and are based on max-type statistics combined with ideas of Krivobokova et al. (2010). For detailed proofs, implementation and applications it is convenient to specify the distribution. We consider area-level Poisson and unit-level logistic models which are widely accepted for studying local poverty rates. In the simulations, all introduced methods show a satisfactory performance. They further indicate that, in our context, our particular specification of the area-level Poisson model outperforms the unit-level logistic modeling on several grounds. First and foremost, we do not require that the number of units in each cluster grows to infinity to prove the consistency of SCIs and MTPs. Secondly, the analysis of the real survey within our framework leads to substantial numerical and computational gains. The estimation of proportion is simpler. What is more, the construction of SCIs under the area-level Poisson takes about 3 minutes using a personal computer, whereas under the unit-level logistic more than 2 days which is almost 1000 times more. Last but not least, our manuscript contributes to the literature comparing the performance of the area-and unit-level models. Nevertheless, EBPs under both settings are not directly comparable as we used different methods and classes of models (GLM versus GLMM); all comparisons should be thus carried out with an additional care. Although our conclusions about the superiority of the area-level model differ considerably from those of, for example, Namazi-Rad and Steel (2015) and Hidioglou and You (2016), it could nevertheless be argued that our results are consistent with a general statistical theory, i.e., a more complicated modelling with random effects and artificially created covariate classes inflate the variability and leads to noisier estimators. Estimation of local poverty rates was extensively discussed in the literature (see the monograph of Pratesi (2016) as well as recent publications of Hobza and Morales (2016) or Boubeta et al. (2016) and references

therein). Despite this interest, no one (to the best of our knowledge) has addressed the issue of simultaneous inference for areas or other clusters when applying GLMMs.

An appropriate measure of the variation of a mixed parameter is the mean squared error (MSE), so that many have studied its estimation in SAE, see Rao and Molina (2015). Since practitioners tend to prefer confidence intervals, over the past fifteen years an increasing number of authors examined different types of confidence (or prediction) intervals. The prominent examples of individual area CI (iCI) under the marginal law (i.e., for randomly selected areas) were put forward by Hall and Maiti (2006a) and Chatterjee et al. (2008). Their iCIs are constructed using resampling techniques, and under certain assumptions, are asymptotically second-order correct for linear mixed models (LMMs).

There is a considerable literature on estimation and testing under GLMM, summarized among others in a review of Tuerlinckx et al. (2006), by Jiang (2007) and Demidenko (2013). Hothorn et al. (2008) develop a framework for MTPs and SCIs for the fixed parameter within LMMs, similarly to Maringwa et al. (2008). Yet, their proposals are hardly related to the problem considered in our paper, i.e., the simultaneous inference with respect to the area parameter, which is a linear combination of fixed and random effects. Ruppert et al. (2003) use the approximation of the volume-of-tube formula of Weyl (1939) to obtain bands for effects under LMM, and Wagler (2014) constructs iCI for EBP. Finally, Ritz et al. (2017) study the asymptotic distribution of fixed parameters coming from different areas. Reluga et al. (2019) propose bootstrap based SCIs and MTPs for the mixed parameter under LMM. Within the same context, Kramlinger et al. (2018) develop a marginal and conditional inference framework using quadratic forms.

We first provide a brief overview of the statistical inference under GLMM, and revisit the definition of the EBP and its MSE. Afterwards, we propose SCI and MTP for the general EBP followed by the derivation of the explicit estimators and their consistency under the specific models. In addition, we present an extensive poverty study together with a reliability study. Our conclusions are drawn in the final paragraph. The appendix include some technical assumptions, derivations and additional results of the simulations. In our context the notion of cluster and area can be used synonymously, we stick henceforth to the latter.

2 Best Prediction For Generalized Linear Mixed Models

Let D be the number of areas with $d \in [D]$, n_d the number of sampled units in each area $j \in [n_d]$, N_d the known population sizes where $[A] = \{1, \dots, A\}$, $n = \sum_{d=1}^D n_d$ and $N = \sum_{d=1}^D N_d$. Suppose that $\{v_d : d = 1, \dots, D\}$ is a set of independent and identically distributed (i.i.d.) random effects with unknown variance δ^2 , $\delta > 0$, which in the literature is often parametrized as $v_d = \delta u_d$ with $u_d \sim N(0, 1)$. The target variable y_{dj} represents the j^{th} sample observation from the d^{th} domain. In full generalization, we assume that the random variables Y_{dj} , conditionally on a random effect u_d , are independent with a probability density function (p.d.f.) from an exponential family $y_{dj}|u_d \sim \text{Exp.Family}(\boldsymbol{\theta})$

$$y_{dj}|u_d \sim \text{indep. } g_{Y_{dj}|u_d}(y_{dj}|u_d) \quad (1)$$

$$g_{Y_{dj}|u_d}(y_{dj}|u_d, \boldsymbol{\theta}) = \exp\{\varphi^{-1}[y_{dj}\gamma_{dj} - b(\gamma_{dj})] + c(y_{dj}, \varphi)\},$$

where $\boldsymbol{\theta} = (\boldsymbol{\beta}^t, \delta, \varphi)^t$ with δ a variability parameter (see above), $\boldsymbol{\beta} = (\beta_1, \dots, \beta_p)^t$ regression parameters of auxiliary variables $\mathbf{x}_{dj} = (x_{dj1}, \dots, x_{djp})^t$ for which typically $x_{dj1} = 1, \forall j \in [n_d]$ and $\forall d \in [D]$. Further, γ_{dj} and φ are a canonical (or natural) and a scale parameter respectively. There exists a link function M which relates a conditional expected value $\mathbb{E}[Y_{dj}|u_d]$ to a linear mixed model and the natural parameter $\gamma_{dj} = M(\mathbb{E}[Y_{dj}|u_d]) = \mathbf{x}_{dj}^t \boldsymbol{\beta} + \delta u_d$. We define $\mathbf{y}_d = (y_{d1}, \dots, y_{dn_d})^t$ for all $d \in [D]$ as a vector of outcomes and $\mathbf{y} = (\mathbf{y}_1^t, \dots, \mathbf{y}_D^t)^t$. A conditional p.d.f. of \mathbf{y} and the likelihood contribution from each area d is given by

$$\mathcal{L}_d(\boldsymbol{\theta}) := f_d(\mathbf{y}_d|\boldsymbol{\theta}) = \int g_d(\mathbf{y}_d|u_d, \boldsymbol{\theta})h(u_d)du_d = \int \prod_{j=1}^{n_d} g_{dj}(y_{dj}|u_d, \boldsymbol{\theta})h(u_d)du_d, \quad (2)$$

where $\boldsymbol{\theta}$ can be derived from

$$\mathcal{L}(\boldsymbol{\theta}) := \prod_{d=1}^D \mathcal{L}_d(\boldsymbol{\theta}) = \prod_{d=1}^D \int \prod_{j=1}^{n_d} g_{dj}(y_{dj}|u_d, \boldsymbol{\theta})h(u_d)du_d.$$

In case of area-level models $n_d = 1$, and (2) simplifies accordingly. For a concise presentation, we assume that there is a single random effect for each area and consequently the integral in (2) is one-dimensional. The extensions to multidimensional random effects follow immediately with some changes of notations and more complicated computation.

Finding an analytical solution to (2) might be difficult due to the integral if it cannot be further simplified. In such case one evaluates the integral using numerical methods such as Laplace approximation (LA) (De Bruijn, 1981), Gaussian quadrature (GQ) (Naylor and Smith, 1982) or adaptive GQ (AGQ) (Pinheiro and Bates, 1995). An alternative is the quasi-likelihood (see, e.g., Stiratelli et al. (1984) or Breslow and Clayton (1993)) which suffers from a non-decreasing bias (Tuerlinckx et al., 2006). Another alternative is the method of moments estimation of Jiang (1998b).

Since we consider a predicting problem of possibly non-linear mixed effects $\zeta_d = \zeta_d(\boldsymbol{\beta}, u_d)$, we use the best predictor (BP) $\tilde{\zeta}_d = \tilde{\zeta}_d(\boldsymbol{\theta})$ which is defined as a conditional expected value

$$\tilde{\zeta}_d := \mathbb{E}[\zeta_d(\boldsymbol{\beta}, u_d)|\mathbf{y}] = \mathbb{E}[\zeta_d(\boldsymbol{\beta}, u_d)|\mathbf{y}_d] = \frac{\int \zeta_d(\boldsymbol{\beta}, u_d)g_d(\mathbf{y}_d|u_d, \boldsymbol{\theta})h(u_d)du_d}{\int g_d(\mathbf{y}_d|u_d, \boldsymbol{\theta})h(u_d)du_d}. \quad (3)$$

Simplification of (3) is possible by choosing the p.d.f. of u_d accordingly. If we replace $\boldsymbol{\theta}$ by a consistent estimator, we obtain the empirical best predictor (EBP) $\hat{\zeta}_d := \tilde{\zeta}_d(\hat{\boldsymbol{\theta}})$. It is worth mentioning that in order to obtain the consistency for a random and fixed effect we need to assume that $n_d \rightarrow \infty$ for each $\hat{\zeta}_d, d = 1, \dots, D$ (Jiang and Lahiri, 2001).

When it comes to the estimation of the variability of the EBP $\hat{\zeta}_d$, MSE is by far the most popular one. Well known techniques are the analytical approximation based on a Taylor expansion (Jiang, 2003) and a parametric bootstrap approach (Boubeta et al., 2016; Hobza and Morales, 2016). One has the following MSE decomposition

$$\text{MSE}(\hat{\zeta}_d) = \mathbb{E}[(\tilde{\zeta}_d(\hat{\boldsymbol{\theta}}) - \zeta_d)^2] = \mathbb{E}[(\tilde{\zeta}_d(\hat{\boldsymbol{\theta}}) - \tilde{\zeta}_d(\boldsymbol{\theta}))^2] + \mathbb{E}[(\tilde{\zeta}_d(\boldsymbol{\theta}) - \zeta_d)^2] =: g_{2d} + g_{1d}. \quad (4)$$

This decomposition neither depends on the distributional assumption of \mathbf{y}_d nor on the p.d.f. of the random effects. Instead, it can be derived applying solely the law of iterated expectations. Details can be found in e.g., Jiang (2003), Boubeta et al. (2016), Hobza and Morales (2016) and our Appendix B. The analytical formulas of MSE estimators are model dependent. Bootstrap based estimators are versatile, and its general technique to obtain them does not vary with the model assumed. We define a direct bootstrap estimator by

$$\text{MSE}_B^*(\hat{\zeta}_d) = \text{MSE}^*(\hat{\zeta}_d^*) = \mathbb{E}[(\hat{\zeta}_d^* - \zeta_d^*)^2] \approx B_1^{-1} \sum_{b_1=1}^{B_1} \left(\hat{\zeta}_d^{*(b_1)} - \zeta_d^{*(b_1)} \right)^2 =: \text{mse}_B(\hat{\zeta}_d), \quad (5)$$

which is a bootstrap equivalent of (4). In their paper, Hall and Maiti (2006b) pointed out that (5) is a first-order correct estimator, and proposed a double bootstrap providing a second-order unbiased MSE estimator. This involves a second-stage bootstrap of the MSE by selecting B_2 bootstrap replicates from each first-stage bootstrap sample:

$$\begin{aligned} \text{MSE}_{B_2}^*(\hat{\zeta}_d) &= \text{MSE}_{B_2}^*(\hat{\zeta}_d^{**}) = \mathbb{E}^{**} \left[(\hat{\zeta}_d^{**} - \zeta_d^{**})^2 \right] \\ &\approx B_1^{-1} B_2^{-1} \sum_{b_1=1}^{B_1} \sum_{b_2=1}^{B_2} \left(\hat{\zeta}_d^{**(b_1 b_2)} - \zeta_d^{**(b_1 b_2)} \right)^2 =: \text{mse}_{B_2}(\hat{\zeta}_d). \end{aligned}$$

The double bootstrap bias corrected MSE estimator is defined as

$$\text{MSE}_{BC}^*(\hat{\zeta}_d) = 2\text{MSE}_B^*(\hat{\zeta}_d) - \text{MSE}_{B_2}^*(\hat{\zeta}_d) \approx 2\text{mse}_B(\hat{\zeta}_d) - \text{mse}_{B_2}(\hat{\zeta}_d), \quad (6)$$

where $\mathbb{E} \left[\text{MSE}_{BC}^*(\hat{\zeta}_d) \right] = \text{MSE}(\hat{\zeta}_d) + o(D^{-1})$. However, in this article we do not aim for a precise estimation of the variability of EBP, but the construction of narrow SCIs and reliable MTPs. It turns out that for doing this, the use of an estimate of g_{1d} as defined in (4) yields better results (see Section 4) than using an estimate of the MSE, similarly as in Chatterjee et al. (2008) under LMMs. In what follows we describe two important examples of GLMMs to study local poverty levels.

2.1 A new Area-level Poisson Model

The area-level Poisson model is widely applied for modeling counts, but usually with normally distributed random effects. We propose a different formulation which results in an importantly simpler expressions that permit yielding a better numerical performance. Under this model we assume that $\zeta_d := \mu_d^P$ and

$$y_d | u_d \sim \text{Pois}(\mu_d^P), \quad d = 1, \dots, D, \quad \text{where } \mu_d^P > 0, \quad n_d = 1 \quad \forall d \in [D],$$

with canonical parameter $\log \mu_d^P = \mathbf{x}_d^t \boldsymbol{\beta} + u_d$, $d = 1, \dots, D$, for which we suppose $w_d := \exp(u_d) \sim \text{Gamma}(\delta, \delta)$ such that $\mathbb{E}[y_d | u_d] = \mu_d^P = \lambda_d w_d = \exp(\mathbf{x}_d^t \boldsymbol{\beta}) w_d = \exp(\mathbf{x}_d^t \boldsymbol{\beta} + u_d)$, cf. Lawless (1987). The main advantage of our formulation is the tractability of the likelihood and the marginal

distribution, that is

$$\begin{aligned}
\mathcal{L}^P(\boldsymbol{\theta}) &:= f^P(\mathbf{y}|\boldsymbol{\theta}) = \prod_{d=1}^D \int_0^\infty \frac{\exp(-\mu_d^P) \mu_d^{P y_d}}{y_d!} f(w_d) dw_d \\
&= \prod_{d=1}^D \frac{\lambda_d^{y_d} \delta^\delta \Gamma(y_d + \delta)}{y_d! \Gamma(\delta) (\delta + \lambda_d)^{y_d + \delta}} \int_0^\infty \frac{(\delta + \lambda_d)^{y_d + \delta} \exp(-(\delta + \lambda_d)w_d) w_d^{y_d + \delta - 1}}{\Gamma(y_d + \delta)} dw_d \\
&= \prod_{d=1}^D \frac{\Gamma(y_d + \delta)}{\Gamma(y_d + 1) \Gamma(\delta)} \left(\frac{\delta}{\delta + \lambda_d} \right)^\delta \left(\frac{\lambda_d}{\delta + \lambda_d} \right)^{y_d}.
\end{aligned} \tag{7}$$

We can see that a gamma p.d.f. is a conjugate to the Poisson, and their mixture gives a negative binomial $y_d \sim NB(\lambda_d, \delta^{-1})$ with $\mathbb{E}[y_d] = \lambda_d$ and $\text{Var}[y_d] = \lambda_d + \delta^{-1} \lambda_d^2$. As usual, the marginal mean of y_d is the same as in the Poisson case, but the random effect increases the variance. The log-likelihood is now proportional to

$$l^P(\boldsymbol{\theta}) = \sum_{d=1}^D \left(\sum_{j=1}^{y_d-1} \log(1 + \delta^{-1}j) + y_d \log \lambda_d - (y_d + \delta) \log(1 + \delta^{-1} \lambda_d) \right), \tag{8}$$

where $\Gamma(b+c)/\Gamma(c) = c(c+1)\dots(c+b-1)$ if $b \geq 1$ and $\sum_{j=1}^{y_d-1} \log(1 + \delta^{-1}j) = 0$ if $y_d - 1 < 0$. A similar expression as in (8) has been used by Lawless (1987) who derived the estimating equations and implemented a scoring algorithm to obtain ML estimate $\hat{\boldsymbol{\theta}}$. For details on derivations, algorithms and implementation see Appendix C.

Suppose that the area-level Poisson model holds for all areas of a population \mathcal{P} of size N partitioned into D subpopulations $\mathcal{P}_1, \mathcal{P}_2, \dots, \mathcal{P}_D$ of sizes N_1, N_2, \dots, N_D . To obtain the estimates of the local poverty, we need to first derive the BP for counts

$$\tilde{\mu}_d^P(\boldsymbol{\theta}) = \mathbb{E}[\mu_d^P | y_d] = \frac{\int_0^\infty \lambda_d w_d g(y_d | w_d) h(w_d) dw_d}{\int_0^\infty g(y_d | w_d) h(w_d) dw_d} = \frac{A_d^P(y_d, \boldsymbol{\theta})}{C_d^P(y_d, \boldsymbol{\theta})} = \frac{\lambda_d (y_d + \delta)}{(\lambda_d + \delta)} =: \psi_d^P(y_d, \boldsymbol{\theta}). \tag{9}$$

The last equality follows from the conjugacy of gamma p.d.f. to Poisson, while

$$\begin{aligned}
A_d^P &= \int_0^\infty \lambda_d w_d \frac{\exp(-\lambda_d w_d) \lambda_d^{y_d} w_d^{y_d} \delta^\delta w_d^{\delta-1} \exp(-w_d \delta)}{y_d! \Gamma(\delta)} dw_d \\
&= \frac{\lambda_d^{y_d+1} \delta^\delta \lambda_d \Gamma(y_d + 1 + \delta)}{\Gamma(\delta) y_d! (\lambda_d + \delta)^{y_d+1+\delta}} \int_0^\infty \frac{w_d^{(y_d+1+\delta)-1} \exp[-(\lambda_d + \delta)w_d] (\lambda_d + \delta)^{y_d+1+\delta}}{\Gamma(y_d + 1 + \delta)} dw_d \\
&= \frac{\lambda_d^{y_d+1} \delta^\delta \Gamma(y_d + 1 + \delta)}{\Gamma(\delta) y_d! (\lambda_d + \delta)^{y_d+1+\delta}}.
\end{aligned}$$

EBP $\hat{\mu}_d^P$ is obtained by replacing the vector of unknown parameters $\boldsymbol{\theta}$ in (9) by a consistent estimator $\hat{\boldsymbol{\theta}}$ whereas the estimate of poverty is given by $\hat{\mu}_d^P = \hat{\mu}_d^P / N_d$. Observe that under area-level Poisson model $\varphi = 1$, and thus $\boldsymbol{\theta} = (\boldsymbol{\beta}, \delta)$. It is also worth mentioning that $\hat{\mu}_d^P$ is an estimator of count of the people below the poverty level in an area d , therefore we need to divide this estimate by the total number of people N_d in this area, $d = 1, \dots, D$. What is more, it is a

common practice to replace N_d with its estimator as the former is usually unknown, see the first paragraph of Section 5 and equation (27).

Regarding the variability of EBP within this modeling framework, we first derive an analytical plug-in MSE estimator. From decomposition (4) it follows

$$g_{1d} := \kappa_{1d}(\boldsymbol{\theta}) - \kappa_{2d}(\boldsymbol{\theta}) \quad \hat{g}_{1d} = \kappa_{1d}(\hat{\boldsymbol{\theta}}) - \hat{\kappa}_{2d}(\hat{\boldsymbol{\theta}}), \quad d \in [D], \quad (10)$$

with $\kappa_{1d}(\boldsymbol{\theta}) = \frac{\lambda_d^2(\delta + 1)}{\delta}$ and $\kappa_{2d}(\boldsymbol{\theta}) = \sum_{j=0}^{\infty} \frac{\lambda_d^2(j + \delta)^2}{(\lambda_d + \delta)^2} P(y_d = j)$.

Note that $\hat{\kappa}_{2d}$ refers to κ_{2d} with an infinite series truncated at a very large term and $\boldsymbol{\theta}$ replaced by $\hat{\boldsymbol{\theta}}$. On the other hand, to estimate κ_{1d} we need only the latter. An analytical plug-in estimator and its practical versions are

$$\text{MSE}_P(\tilde{\mu}_d^P) = g_{P1d} + \frac{1}{D} c_d(\boldsymbol{\theta}) + o(1/D) \quad \text{and} \quad \text{mse}_P(\hat{\mu}_d^P) = \hat{g}_{P1d} + \frac{1}{D} \hat{c}_d(\hat{\boldsymbol{\theta}}) \quad (11)$$

where

$$c_d = \sum_{j=1}^{\infty} \left(\frac{\partial}{\partial \boldsymbol{\theta}} \psi_d(y_d, \boldsymbol{\theta}) \right)^t \text{Var}_d(\boldsymbol{\theta}) \left(\frac{\partial}{\partial \boldsymbol{\theta}} \psi_d(y_d, \boldsymbol{\theta}) \right) P(y_d = j)$$

$$\text{Var}_d[\boldsymbol{\theta}] = D \mathbb{E} \left[(\hat{\boldsymbol{\theta}} - \boldsymbol{\theta}) (\hat{\boldsymbol{\theta}} - \boldsymbol{\theta})^t \right],$$

and $\hat{c}_d(\boldsymbol{\theta})$ a Monte Carlo approximation of $c_d(\boldsymbol{\theta})$ in which the variance of $\hat{\boldsymbol{\theta}}$ is estimated by bootstrap, see Section 4 equation (26).

2.2 A Unit-level Logit Model

A unit-level logit model is widely applied for binary responses contrary to the area-level model which is applied to model counts. The former has been comprehensively discussed by e.g., Hobza and Morales (2016). In addition, Poisson distribution is a limiting case of the binomial-logit distribution. Under this setting, a p.d.f. of the response variable, conditional on the random effect u_d , is

$$y_{dj} | u_d \sim \text{Bin}(m_{dj}, p_{dj}),$$

where m_{dj} is a known size parameter for a logistic regression, and $u_d \sim N(0, 1)$. For the natural parameter, we suppose

$$\eta_{dj}^B = \log \frac{p_{dj}}{1 - p_{dj}} = \mathbf{x}_{dj}^t \boldsymbol{\beta} + \delta u_d, \quad d = 1, \dots, D, \quad j = 1, \dots, n_d,$$

where

$$p_{dj} = \frac{\exp(\mathbf{x}_{dj}^t \boldsymbol{\beta} + \delta u_d)}{1 + \exp(\mathbf{x}_{dj}^t \boldsymbol{\beta} + \delta u_d)}. \quad (12)$$

In this section we assume that the unit-level logit model holds for all units of a population \mathcal{P} of size N partitioned into D subpopulations \mathcal{P}_d of sizes N_d , $d = 1, \dots, D$. Consider the case when the parameter of interest is $\zeta_d := \mu_d^B = \sum_{j=1}^{N_d} p_{dj}$. The conditional distribution of \mathbf{y} is given by

$$f^B(\mathbf{y}|\boldsymbol{\theta}) = \prod_{d=1}^D \int_{\mathbb{R}} \prod_{j=1}^{n_d} \binom{m_{dj}}{y_{dj}} (2\pi)^{-1/2} p_{dj}^{y_{dj}} (1 - p_{dj})^{m_{dj} - y_{dj}} \exp(-u_d^2/2) du_d. \quad (13)$$

Like for our area-level model, $\varphi = 1$ and therefore $\boldsymbol{\theta} = (\boldsymbol{\beta}^t, \delta)$. Combining (12) and (13)

$$\begin{aligned} \mathcal{L}^B(\boldsymbol{\theta}) &:= f^B(\mathbf{y}|\boldsymbol{\beta}, \delta) = (2\pi)^{-D/2} \prod_{d=1}^D \int_{\mathbb{R}} \prod_{j=1}^{n_d} \binom{m_{dj}}{y_{dj}} \frac{\exp[y_{dj}(\mathbf{x}_{dj}^t \boldsymbol{\beta} + \delta u_d) - u_d^2/2]}{[1 + \exp(\mathbf{x}_{dj}^t \boldsymbol{\beta} + \delta u_d)]^{m_{dj}}} du_d \\ &= (2\pi)^{-D/2} \prod_{d=1}^D \int_{\mathbb{R}} \exp \left\{ \sum_{j=1}^{n_d} \log \binom{m_{dj}}{y_{dj}} + \sum_{j=1}^{n_d} y_{dj} (\mathbf{x}_{dj}^t \boldsymbol{\beta} + \delta u_d) \right. \\ &\quad \left. - \frac{u_d^2}{2} - \sum_{j=1}^{n_d} m_{dj} \log[1 + \exp(\mathbf{x}_{dj}^t \boldsymbol{\beta} + \delta u_d)] \right\} du_d. \end{aligned} \quad (14)$$

Direct maximization of the log-likelihood is cumbersome due to the integral which cannot be easily simplified. One can approximate the integral using AGQ, or the integrand applying Laplace approximation. In what follows we proceed with the former as it is a higher order version of the latter, i.e., it provides smaller approximation error (Bianconcini, 2014). Our approach concerning estimation might be considered as a comparative study to Hobza and Morales (2016). Regarding EBP and its variability, our derivations proceed in the same lines as in Hobza and Morales (2016). Therefore, some details are deferred to Appendix D, others can be found directly in their paper.

Our goal is to obtain the best predictor $\tilde{p}_{dj}(\boldsymbol{\theta})$ of p_{dj} and of the sum of probabilities $\tilde{\mu}_d^B = \sum_{j=1}^{N_d} \tilde{p}_{dj}$. If we dispose of information on each unit of the population, we can proceed with the estimations of these quantities. In many real data applications, the auxiliary information is available only for the sample units. Nevertheless, we can still use the sample to estimate the population quantity of interest if we follow the suggestion of Hobza and Morales (2016): Suppose we use only the categorical covariates which take a finite number of values, say $\mathbf{x}_{dj} \in \{\mathbf{z}_1, \dots, \mathbf{z}_L\} \forall d, \forall j$ with \mathbf{z}_l denoting the resulting classes. Then

$$\bar{\mu}_d^B = \frac{\mu_d^B}{N_d}, \quad \mu_d^B = \sum_{j=1}^{N_d} p_{dj} = \sum_{l=1}^L N_{dl} r_{dl}, \quad r_{dl} = \frac{\exp(\mathbf{z}_l \boldsymbol{\beta} + \delta u_d)}{1 + \exp(\mathbf{z}_l \boldsymbol{\beta} + \delta u_d)} \quad (15)$$

where $N_{dl} = \#\{l \in \mathcal{P}_d : \mathbf{x}_{dj} = \mathbf{z}_l\}$ is a known size of the covariate class \mathbf{z}_l in area d . Hobza and Morales (2016) derived BPs $\tilde{\mu}_d^B(\boldsymbol{\theta})$ and EBP $\hat{\mu}_d^B(\hat{\boldsymbol{\theta}})$ for all quantities in (15).

When it comes to the MSE estimation, Jiang (2003) suggested an analytical derivation using a Taylor expansion based on the estimators obtained by the method of simulated moments. Though consistent, Hobza and Morales (2016) pointed out that the analytical MSE is not practical for medium- and large-cluster sizes because it requires the iterative search of the $\binom{n_d}{j}$ subsets of size j , which equals to around 19×10^4 already for $n_d = 20$ and $j = 10$. While this calculation would

be doable in the simulation study with fixed n_d , it becomes particularly cumbersome for a great majority of data problems, because it is not unusual to have at least one cluster with $n_d > 20$. For this reason we follow the suggestion of these authors, and use a parametric bootstrap MSE estimator which is less computational intensive and a performance comparable with the analytical MSE estimate.

3 Simultaneous Intervals and Multiple Testing

Little research has been carried out on simultaneous inference under GLMM, and even less assuming this model in SAE despite its indisputable relevance. We start with the construction of simultaneous prediction intervals for $\hat{\zeta}_d$, accounting for the effect of the estimates for other areas. This implies that we need to find a confidence region $\mathcal{I}_{1-\alpha}$ such that $P(\zeta_d \in \mathcal{I}_{1-\alpha} \forall d \in [D]) = 1 - \alpha$. In spite of dealing with GLMM, we can apply ideas of Reluga et al. (2019), and consider

$$\alpha = P\left(\left|\hat{\zeta}_d - \zeta_d\right| > q_{S_0}(1 - \alpha)\hat{\sigma}(\hat{\zeta}_d) \forall d \in [D]\right) = P\left(\max_{d=1, \dots, D} \left|\frac{\hat{\zeta}_d - \zeta_d}{\hat{\sigma}(\hat{\zeta}_d)}\right| > q_{S_0}(1 - \alpha)\right), \quad (16)$$

where $\hat{\sigma}(\hat{\zeta}_d)$ is some estimate of variability of the EBP. Then the construction of SCIs boils down to the estimation of a high quantile $q_{S_0}(1 - \alpha)$ from the p.d.f. of

$$S_0 = \max_{d=1, \dots, D} |S_{0d}|, \quad \text{with } S_{0d} = \frac{\hat{\zeta}_d - \zeta_d}{\hat{\sigma}(\hat{\zeta}_d)}, \quad \forall d \in [D], \quad (17)$$

$$q_{S_0}(1 - \alpha) := \inf\{t \in \mathbb{R} : P(S_0 \leq t) \geq 1 - \alpha\}. \quad (18)$$

Once one has (18), the construction of SCI follows straightforwardly

$$\mathcal{I}_{1-\alpha}^S = \times_{d=1}^D \mathcal{I}_{d,1-\alpha}^S, \quad \text{where } \mathcal{I}_{d,1-\alpha}^S = \left[\hat{\zeta}_d \pm q_{S_0}(1 - \alpha) \times \hat{\sigma}(\hat{\zeta}_d)\right], \quad (19)$$

where \times denotes a generalized Cartesian product and $\mathcal{I}_{1-\alpha}^S$ covers all ζ_d with a probability $1 - \alpha$. In contrast, iCI is given as

$$\mathcal{I}_{d,1-\alpha}^{iCI} = \left[\hat{\zeta}_d \pm q_{S_{0d}}(1 - \alpha) \times \hat{\sigma}(\hat{\zeta}_d)\right] \quad \forall d \in [D], \quad (20)$$

where $q_{S_{0d}}(1 - \alpha)$ is defined analogously to $q_{S_0}(1 - \alpha)$. It is worthwhile mentioning that by construction, iCIs do not cover ζ_d for at least $100\alpha\%$ of all areas.

Even though the interval in (19) is attractive, it is not operational because we do not know the true value of the non-linear mixed effect. Under LMM, Reluga et al. (2019) proposed two practical methods to build such intervals: Monte Carlo approximation and bootstrap bands. Since the former is tightly related to the normality assumption, we restrain ourselves to the latter approach which implies an approximation of the distribution of (17) using parametric bootstrap, that is

$$S_B^{(b_1)} = \max_{d=1, \dots, D} \left|S_{Bd}^{(b_1)}\right|, \quad S_{Bd}^{(b_1)} = \frac{\hat{\zeta}_d^{*(b_1)} - \zeta_d^{*(b_1)}}{\hat{\sigma}^{*(b_1)}(\hat{\zeta}_d^*)} \quad (21)$$

where $b_1 = 1, \dots, B_1$. Then a critical value is a high quantile

$$q_{S_B}(1 - \alpha) := \inf\{t \in \mathbb{R} : \mathbb{P}(S_B \leq t | (\mathbf{y}, \mathbf{X})) \geq 1 - \alpha\}$$

is approximated by a $[(1 - \alpha)B_1 + 1]^{th}$ order statistic of the $S_B^{(b_1)}$. Thus, the bootstrap equivalent of (19) is given by

$$\mathcal{I}_{1-\alpha}^B = \prod_{d=1}^D \mathcal{I}_{d,1-\alpha}^B, \quad \text{where} \quad \mathcal{I}_{d,1-\alpha}^B = \left[\hat{\zeta}_d \pm q_{S_B}(1 - \alpha) \times \hat{\sigma}(\hat{\zeta}_d) \right]. \quad (22)$$

An alternative approach to the construction of SCI would be to focus on a non-studentized statistic. Since we do not have to estimate the variability parameter, this implementation is simpler. Nonetheless, already DiCiccio and Efron (1996) pointed out, that the lack of studentization results in slower convergence rates. In fact, application of the non-studentized SCIs did not yield satisfactory results, therefore we decided not to include it.

Our methodology is readily applicable for hypothesis testing. Consider the problem

$$H_0 : \mathbf{B}\boldsymbol{\zeta} = \mathbf{b} \quad \text{vs.} \quad H_1 : \mathbf{B}\boldsymbol{\zeta} \neq \mathbf{b}, \quad (23)$$

where $\mathbf{B} \in \mathbb{R}^{D' \times D}$ matrix with $D' \leq D$ and $\mathbf{b} \in \mathbb{R}^{D'}$. The test based on the max-type statistic t_H rejects H_0 at the α -level if $t_H \geq q_{H_0}(1 - \alpha)$ with $q_{H_0}(1 - \alpha) := \inf\{t \in \mathbb{R} : \mathbb{P}(S_{H_0} \leq t) \geq 1 - \alpha\}$ and

$$t_H := \max_{d=1, \dots, D'} |t_{H_d}|, \quad S_{H_0} := \max_{d=1, \dots, D} |S_{H_0d}|, \quad t_{H_d} = \frac{\hat{\zeta}_d^H - b_d}{\hat{\sigma}(\hat{\zeta}_d^H)}, \quad S_{H_0d} = \frac{\zeta_d^H - b_d}{\hat{\sigma}(\zeta_d^H)}, \quad (24)$$

where $\boldsymbol{\zeta}^H = (\zeta_1^H, \dots, \zeta_{D'}^H)^t := \mathbf{B}\boldsymbol{\zeta} \in \mathbb{R}^{D'}$ and $\hat{\boldsymbol{\zeta}}^H$ its estimated counterpart. In practice we might use such a test to examine differences between area characteristic.

We conclude by providing consistency and asymptotic coverage probabilities of SCI. Note that the speed of convergence of $\hat{\boldsymbol{\theta}}$ and $\hat{\boldsymbol{\theta}}^*$ is related to the method of estimation. We consider two different techniques, that is ML and AGQ(q), with q number of quadrature points. In the study of local poverty rates, we employ the former under the area-level model, and the latter under unit-level model. Consistency of $\hat{\boldsymbol{\theta}}$ obtained using ML is a well established result in the statistical literature, see, for example Schervish (2012), whereas AGQ(q) is proved by Bianconcini (2014). Last but not least, we consider a parametric bootstrap. For its specific implementation under the area-level Poisson model, see the algorithm in Section 4.

Proposition 1. *Under assumptions 1-5 from Appendix A it holds that:*

$$\mathbb{E}^*(y_{dj}^*) - \mathbb{E}(y_{dj}) = o_{P^*}(1) \quad \text{and} \quad \text{Var}^*(\mathbf{y}_d^*) - \text{Var}(\mathbf{y}_d) = [o_{P^*}(1)]_{n_d \times n_d}$$

Furthermore, we have:

1. for ML estimation: $\|\hat{\boldsymbol{\theta}}^* - \hat{\boldsymbol{\theta}}\| = O_{P^*}(n^{-1/2})$,
2. for AGQ(q)-ML estimation: $\|\hat{\boldsymbol{\theta}}^* - \hat{\boldsymbol{\theta}}\| = O_{P^*}[\max\{(n^{-1/2}), \min(n_d)^{[-q/3+1]}\}]$, where q is the number of quadrature points.

Proof. Let $y_{dj}^* \sim \text{Exp.Family}(\boldsymbol{\theta})$. If u_d^* is sampled from a suitable distribution, then we have $\gamma_{dj}^* = M(\mathbb{E}(y_{dj}^*|u_d)) = x_{dj}^t \hat{\boldsymbol{\beta}} + u_d^*$. Furthermore, $\text{Var}^*(\mathbf{y}_d^*) = \text{Var}^*(\mathbb{E}^*(\mathbf{y}_d^*|u_d^*)) + \mathbb{E}^*(\text{Var}^*(\mathbf{y}_d^*|u_d^*))$. The first part of the Proposition follows from the way we generate the random effects as well as results on the consistency of $\hat{\boldsymbol{\theta}}$. To show the second part we consider a general score equation and replace \mathbf{y} with \mathbf{y}^* and set $\boldsymbol{\theta} = \hat{\boldsymbol{\theta}}$, i.e., $S^*(\boldsymbol{\theta}) = \frac{\partial l^*(\hat{\boldsymbol{\theta}})}{\partial \boldsymbol{\theta}} = \sum_{d=1}^D \frac{\partial \log f_d(\mathbf{y}_d^*|\hat{\boldsymbol{\theta}})}{\partial \boldsymbol{\theta}} = 0$. Then $\mathbb{E}^*[S^*(\boldsymbol{\theta})] = 0$ at $\boldsymbol{\theta} = \hat{\boldsymbol{\theta}}$ which yields consistency of $\hat{\boldsymbol{\theta}}^*$.

Given these results, we can derive the consistency of $\mathcal{I}_{1-\alpha}^B$ based on some general ideas from the extreme value theory and the asymptotic expansion of the standardized statistic, similar to Chatterjee et al. (2008). In the following demonstration we assume $\hat{\sigma}(\hat{\zeta}_d) = \sqrt{\hat{g}_{1d}(\hat{\zeta}_d)}$, but a similar result is immediate for $\hat{\sigma}(\hat{\zeta}_d) = \sqrt{\text{mse}_{(\cdot)}(\hat{\mu}_d^P)}$ with some heavier derivations where (\cdot) stands for different types of estimators. If no confusion is possible, we use $q := q_{S_0}(1 - \alpha)$ and denote the cumulative distribution function (c.d.f.) of S_{0d} and S_{Bd} by $G_d(w) = P(S_{0d} \leq w)$ and $G_d^*(w) = P(S_{Bd} \leq w)$. In Appendix C.3 we provide for both short asymptotic expansions. Define $(S_{0(d+1)}, \dots, S_{0(2D)}) = (-S_{01}, \dots, -S_{0D})$ and observe that $\max_{d=1, \dots, D} |S_{0d}| = \max_{d=1, \dots, 2D} (S_{01}, \dots, S_{0D}, -S_{01}, \dots, -S_{0D})$. From (16) it follows

$$\mathcal{T}_D(q) = P(S_0 \leq q) = P(S_{01} \leq q, \dots, S_{0D} \leq q, -S_{01} \leq q, \dots, -S_{0D} \leq q) = \prod_{d=1}^{2D} G_d^{2D}(q) \quad (25)$$

for $D \in \mathbb{N}$. As $D \rightarrow \infty$, unless standardized, the distribution in (25) would converge to 0 or 1. In Appendix C.3 we showed that $G_d(w)$ is asymptotically normally distributed. Therefore $P(S_0 \leq q) \approx \Phi^{2D}(q)$; it is well known the standard normal distribution is in the domain of attraction of the Gumbel law, that is

$$\lim_{D \rightarrow \infty} \Phi^{2D}(q/b_D + b_D) = \exp(\exp(-q)), \quad \text{for all } q \in \mathbb{R}$$

where b_D , is a sequence of constants (their explicit form can be found in Theorem 1.5.3 in Leadbetter et al. (2012)). The main drawback of this approximation is a poor rate its convergence – already Fisher and Tippett (1928) noticed that it is not faster than $1/\log(D)$. An application of the bootstrap statistic provides thus an immediate remedy to this issue. Notice that a similar representation holds for S_B , replacing P with P^* and true fixed and random parameters with their estimates. Application of Poyla’s theorem which combines the convergence in distribution with a convergence in sup norm results in the second proposition.

Proposition 2. *Under assumptions 1-5 from Appendix A and above arguments, we have that*

$$\sup_{w \in \mathbb{R}} |\mathcal{T}_D(w) - \mathcal{T}_D^*(w)| \rightarrow 0$$

Corollary 1. *Proposition 2 implies that*

$$P(\zeta_d \in \mathcal{I}_{1-\alpha}^B \forall d \in [D]) \rightarrow 1 - \alpha.$$

4 Empirical Reliability Study

We performed an intensive simulation study in order to assess the reliability of the developed methods in finite samples. More specifically, we considered simulation scenarios in which we developed SCI for EBP under the area-level Poisson model from Section 2.1 and the unit-level binomial model from Section 2.2. In our reliability analysis we examined the empirical performance of the different estimators. We quantified relative bias (RBIAS) and relative root-MSE (RRMSE) of fixed effects β and variability parameter δ . Secondly, EBP $\hat{\mu}_d^P$ and $\hat{\mu}_d^B$, $d = 1, \dots, D$, were evaluated looking at bias, average absolute bias, MSE and average MSE. Since they did not show any atypical patterns, their detailed expressions and results for both area- and unit-level model are deferred to the Appendix C.4 and D.4. Regarding SCIs, we calculated an empirical coverage probability (ECP)

$$ECP = \frac{1}{K} \sum_{k=1}^K \mathbb{1}\{\zeta_d^{(k)} \in \mathcal{I}_{1-\alpha}^S \forall d \in [D]\},$$

an average width over the areas of SCI

$$WS = \frac{1}{DK} \sum_{d=1}^D \sum_{k=1}^K \omega_d^{(k)}, \quad \omega_d^{(k)} = 2q_{(\cdot)}^{(k)}(1 - \alpha) \hat{\sigma}^{(k)}(\hat{\zeta}_d),$$

and a variation of width

$$VS = \frac{1}{D(K-1)} \sum_{d=1}^D \sum_{k=1}^K \left(\omega_d^{(k)} - \bar{\omega}_d \right)^2, \quad \bar{\omega}_d = \frac{1}{K} \sum_{k=1}^K \omega_d^{(k)}, \quad d = 1, \dots, D,$$

where K is the number of simulation runs.

4.1 Finite sample performance of SCI under the area-level model

Under the area-level Poisson model we assumed that $y_d \sim Poiss(\mu_d^P)$, $\mu_d^P = \lambda_d w_d$, $\lambda_d = \exp(\beta_0 + \beta_1 x_{1d} + \beta_2 x_{2d} + \beta_3 x_{3d} + \beta_4 x_{4d})$, $w_d \sim Gamma(\delta, \delta)$. The model parameters and the sample sizes are taken from our application, see Section 5, i.e., we set $\beta_0 = 10.038$, $\beta_1 = 7.747$, $\beta_2 = -3.136$, $\beta_3 = 11.317$, $\beta_4 = -2.466$ and $\delta = 2.480$. We studied the performance for different sample sizes, namely for $D = 52$ using exactly the original sample, for $D = 26$ using randomly selected areas without replacement, and for $D = 78$ which was composed of the original sample plus 26 randomly selected areas (i.e., each area enters at most twice). The parameter of interest is the area proportion of individuals below a poverty level $\bar{\mu}_d^P = \mu_d^P / N_d$ with N_d a true sample size of the area; its EBP is given by (9). The number of the first and second stage bootstraps are $B_1 = 1000$ and $B_2 = 1$. For each of the three cases we generated $K = 1000$ samples with the same areas and fixed covariates, but randomly drawn w_d and y_d . In what follows we describe the exact algorithm for constructing SCI and iCI in each simulation run.

1. Fit the model to the data and obtain consistent estimators $\hat{\theta} = (\hat{\beta}, \hat{\delta})$.

2. For $b_1 = 1, \dots, B_1$ bootstrap samples generate $w_d^{*(b_1)} \sim \text{Gamma}(\hat{\delta}, \hat{\delta})$ *i.i.d.* and set

$$\mu_d^{P*(b_1)} = \hat{\lambda}_d w_d^{*(b_1)} \quad \text{and} \quad y_d^{*(b_1)} \sim \text{Poisson}(\mu_d^{P*(b_1)}).$$

3. For each bootstrap sample calculate $\hat{\boldsymbol{\theta}}^{*(b_1)}$, $\hat{\mu}_d^{P*(b_1)}(\hat{\boldsymbol{\theta}}^{*(b_1)})$ and $AD_{P,d}^{(b_1)} = \left| \hat{\mu}_d^{P*(b_1)} - \mu_d^{P*(b_1)} \right|$.

(a) For $b_2 = 1, \dots, B_2$ generate samples $w_d^{***(b_1, b_2)} \sim \text{Gamma}(\hat{\delta}^{*(b_1)}, \hat{\delta}^{*(b_1)})$ *i.i.d.* and

$$\mu_d^{P***(b_1, b_2)} = \hat{\lambda}_d^{*(b_1)} w_d^{***(b_1, b_2)} \quad \text{and} \quad y_d^{***(b_1, b_2)} \sim \text{Poisson}(\mu_d^{P***(b_1, b_2)}).$$

(b) For each bootstrap sample calculate $\hat{\boldsymbol{\theta}}^{***(b_1, b_2)}$ and $\hat{\mu}_d^{P***(b_1, b_2)}(\hat{\boldsymbol{\theta}}^{***(b_1, b_2)})$

(c) Set $mse_d^{(b_1)} = \frac{1}{B_2} \sum_{b_2=1}^{B_2} \left(\hat{\mu}_d^{P***(b_1, b_2)} - \mu_d^{P***(b_1, b_2)} \right)^2$.

4. Calculate bootstrap estimators $\hat{g}_{1d}(\hat{\boldsymbol{\theta}}^{*(b_1)})$ as in (10),

$$mse_B(\hat{\mu}_d^P) = \frac{1}{B_1} \sum_{b_1=1}^{B_1} \left(\hat{\mu}_d^{P*(b_1)} - \mu_d^{P*(b_1)} \right)^2 \quad \text{and} \quad mse_{BC}(\hat{\mu}_d^P) = 2mse_B(\hat{\mu}_d^P) - \frac{1}{B_1} \sum_{b_1=1}^{B_1} mse_d^{(b_1)}.$$

5. Calculate estimated bootstrap statistic $S_{P,B}$ with the critical value $q_{P,S_E}(1 - \alpha)$ from $\mathbf{S}_{P,B} = (S_{P,B}^{(1)}, \dots, S_{P,B}^{(B_1)})^t$ where

$$S_{P,B}^{(b_1)} = \max_{d=1, \dots, D} \frac{AD_{P,d}^{*(b_1)}}{\hat{\sigma}^{*(b_1)}(\hat{\mu}_d^{P*(b_1)})} \quad \text{and} \quad q_{P,S_E}(1 - \alpha) = Q_{1-\alpha}(\mathbf{S}_{P,B})$$

as well as estimated variance of $\boldsymbol{\theta}$,

$$\widehat{var}(\hat{\boldsymbol{\theta}}) = \frac{1}{B_1} \sum_{b_1=1}^{B_1} (\hat{\boldsymbol{\theta}}^{*(b_1)} - \bar{\boldsymbol{\theta}})(\hat{\boldsymbol{\theta}}^{*(b_1)} - \bar{\boldsymbol{\theta}})^t \quad \text{with} \quad \bar{\boldsymbol{\theta}} = \frac{1}{B_1} \sum_{b_1=1}^{B_1} \hat{\boldsymbol{\theta}}^{*(b_1)}. \quad (26)$$

In a testing context we generate bootstrap samples in Step 2 and obtain critical values from the bootstrap equivalent of S_{H_0} in similar way as in Step 5. Regarding the variability parameters $\hat{\sigma}(\hat{\mu}_d^P)$ and its bootstrap equivalent $\hat{\sigma}^*(\hat{\mu}_d^{*P})$ in Step 5, we compared the performance of SCIs and MPTs for several estimators, i.e., $\hat{\sigma}(\hat{\mu}_d^P) = \sqrt{\hat{g}_{1d}}$ and $\hat{\sigma}^*(\hat{\mu}_d^{*P}) = \sqrt{mse_{(\cdot)}(\hat{\mu}_d^{*P})}$. Furthermore, $mse_{(\cdot)}$ refers to either the plug-in mse_P in (11), the mse_B or mse_{BC} defined in (5) and (6) for a general EBP. Steps 3(a)-(c) refer to the second-stage bootstrap which is only necessary to obtain bias corrected mse_{BC} . Recall that we are interested in poverty rates which are in fact area proportions. The above algorithm is readily applicable for this case. To obtain its estimator, we need to divide the initial parameter of interest by the total size of the cluster, i.e.,

$$\hat{\mu}_d^P = \hat{\mu}_d^P / N_d, \quad \hat{g}_{P1d} = \hat{g}_{P1d} / N_d^2 \quad \text{and} \quad mse_{(\cdot)}(\hat{\mu}_d^P) = mse_{(\cdot)}(\hat{\mu}_d^P) / N_d^2.$$

Table 1 summarizes the performance of our SCIs for $\hat{\mu}_d^P$ constructed using mse_B (B), mse_{BC} (BC), plug-in mse (P), and SCIs using \hat{g}_{1d} (G). All proposed methods show a good ECP already

| ECP (in %) | | | | | WS $\times 10^3$ (VS $\times 10^3$) | | | | |
|------------|------|------|------|------|--------------------------------------|---------------|---------------|---------------|--|
| D | B | BC | P | G | B | BC | P | G | |
| 26 | 95.7 | 95.9 | 95.8 | 95.3 | 24.4 (0.0251) | 24.5 (0.0276) | 24.5 (0.0244) | 23.9 (0.0227) | |
| 52 | 94.7 | 93.7 | 94.9 | 94.6 | 30.3 (0.0303) | 30.3 (0.0343) | 30.4 (0.0294) | 29.8 (0.0282) | |
| 78 | 94.7 | 94.8 | 94.9 | 94.4 | 33.4 (0.0265) | 33.4 (0.0323) | 33.5 (0.0253) | 33.0 (0.0243) | |

Table 1: ECP, WS and VS of different SCIs under the area-level Poisson model. Nominal coverage probability is 95%.

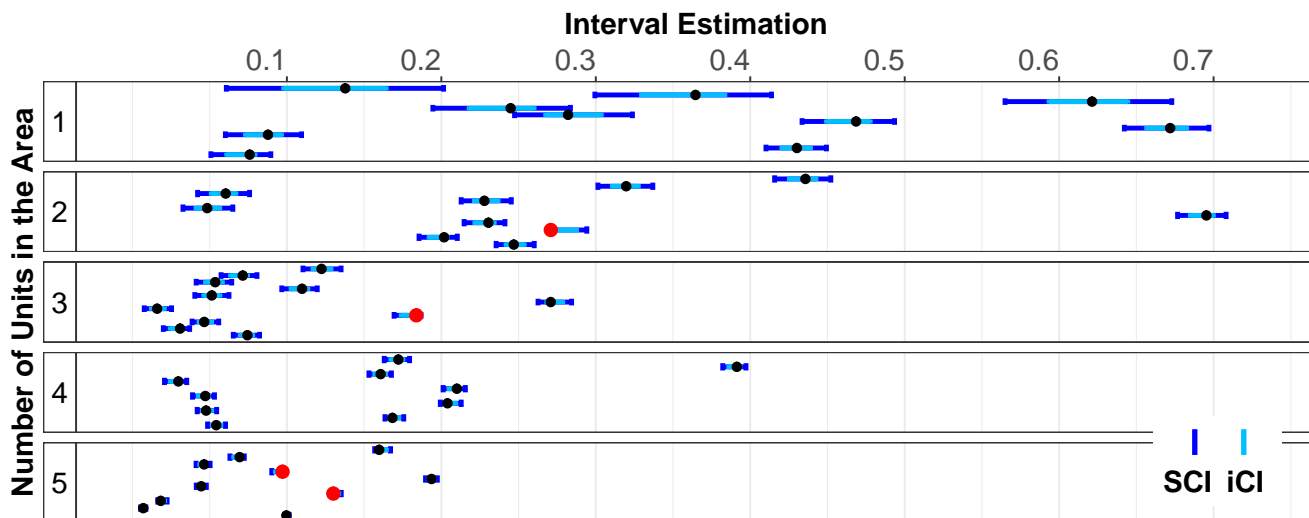


Figure 1: iCI and bootstrap SCI for proportions, $D = 52$. Red dots denote true parameters outside iCI.

for $D = 26$. It is noteworthy that SCIs constructed using a Bonferroni procedure yield very poor results with an unacceptably low ECP (for example, for $D = 52$ and mse_B it was equal to 78%). Therefore, we do not report them. Figure 1 presents 95% SCI and iCI estimates for one, randomly selected simulation. The plot is divided into 5 panels with the first presenting the results for the areas with the fewest observations and the fifth for the most populous areas. The true area proportions are represented with black and red dots. The latter indicate those $\bar{\mu}_d^P$ which are outside of their iCI. It turns out that in this sample four of the true area proportions (i.e., approximately 7.7%) are not contained in their iCI. We obtained similar figures for other simulated samples.

Finally we study the performance of our test (23) introduced in Section 3. Consider $H_0 : \bar{\mu}^P = \mathbf{h}$ versus $H_1 : \bar{\mu}^P = \mathbf{h} + \mathbf{1}_D \Delta$ where $\mathbf{h} := \bar{\mu}$ for the same data generating processes and scenarios as before. Figure 2 shows the empirical power functions of the test based on different variability estimates. We see that there are no visible differences. This is not surprising when comparing it with Table 1 which does not only indicate similar coverage probabilities (close to the nominal level), but also similar WS and VS. For $D = 52$, i.e., the simulations based on the real data, the nominal level of $\alpha = 0.05$ is met almost exactly under H_0 .

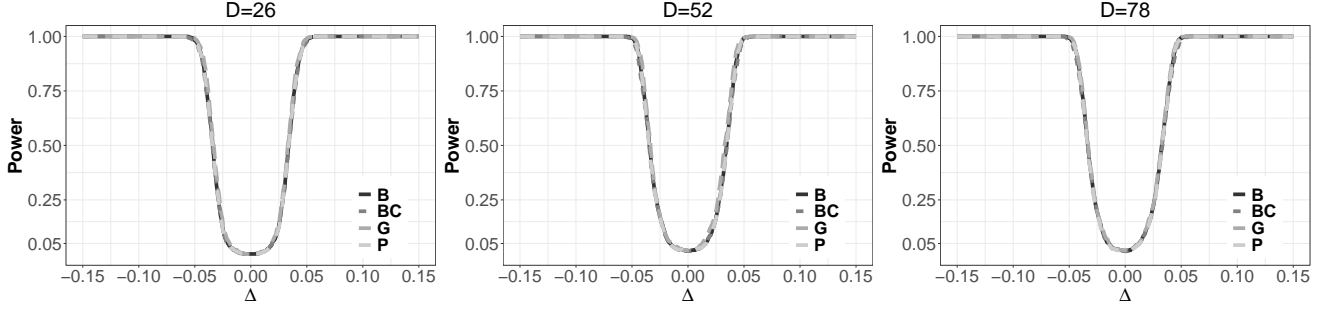


Figure 2: Simulated power for testing $H_0 : \bar{\mu}^P = \mathbf{h}$ versus $H_1 : \bar{\mu}^P = \mathbf{h} + \mathbf{1}_D \Delta$; (left) $D = 26$, (center) $D = 52$, (right) $D = 78$.

4.2 Finite sample performance of SCI under the unit-level model

Under the unit-level model one assumes

$$y_{dj} \sim \text{Bin}(m_{dj}, p_{dj}), \quad p_{dj} = \frac{\exp(\beta_0 + x_{dj1}\beta_1 + x_{dj1}\beta_2 + x_{dj3}\beta_1 + x_{dj4}\beta_2 + \delta u_d)}{1 + \exp(\beta_0 + x_{dj1}\beta_1 + x_{dj1}\beta_2 + x_{dj3}\beta_1 + x_{dj4}\beta_2 + \delta u_d)}, \quad m_{dj} = 1,$$

where p_{dj} is a binomial probability, $u_d \sim N(0, 1)$, and y_{dj} is binary with 1 indicating an individual below a poverty threshold (for details see Section 5). Similarly to the area-level model, the model parameter are taken from our case study, i.e., $\beta_0 = -2.048$, $\beta_1 = 0.989$, $\beta_2 = 0.172$, $\beta_3 = 0.760$, $\beta_4 = 0.100$ and $\delta = 0.348$. Four categorical covariates resulted in 16 covariate classes, namely $\mathbf{x}_{dj} \in \{\mathbf{z}_1, \dots, \mathbf{z}_{16}\}$ for which we needed to estimate N_{dl} , which is done in practice, using (27), $l = 1, \dots, 16$. In our simulation study we consider $D = 52$ with n_d , N_d , \mathbf{x}_{dj} and \mathbf{z}_l as in the case study. As above, we also simulate cases with $D = 26$ and $D = 78$ areas (selected as above); within each of them we then sample with replacement n_d units (i.e., 26 newly sampled areas contain different units in comparison to the original sample). It is worth mentioning that our setting is not optimal from the asymptotic point of view, see discussion in Section 2. The area-level model is a cleverly modeled exception from this asymptotic regime. Nonetheless, the simulation setting from our reliability study is more common in practice. The parameter of interest is the area poverty proportion $\bar{\mu}_d^B$ defined in (15). Since the original sample size is $n = 23628$, under the unit-level model we restricted ourselves to $K = 200$, $B_1 = 500$ and B_2 as for the area-level model. As far as the algorithm for constructing SCI and iCI is taken into consideration, it follows almost the same steps as the procedure described in Section 4.1. We only need to replace the Poisson distribution with binomial and normal random effects with gamma distributed random effects. For the sake of brevity, the exact algorithm under the unit-level model was deferred to Appendix D.4. Table 2 presents the performance of SCIs constructed using mse_B (B) and mse_{BC} (BC). Although the coverage probability is clearly worse than for the area-level model in Table 1, which is not surprising with fixed number of units in areas, it still osculates around 92 – 94%. The average width of the intervals is the most striking difference. Even though these results differ from some earlier studies (Hidioglou and You, 2016), they are consistent with general statistical theory. EBP under the unit-level model is estimated using 16 different covariate classes which requires the estimation of the size of 16 times more artificially created clusters. What is more, GLMM

| ECP (in %) | | | WS $\times 10^3$ (VS $\times 10^3$) | |
|------------|------|----|--------------------------------------|----------------|
| D | B | BC | B | BC |
| 26 | 94 | 93 | 134.0 (0.1928) | 135.0 (0.2683) |
| 52 | 93.5 | 93 | 150.3 (0.1390) | 150.9 (0.1886) |
| 78 | 93 | 92 | 153.9 (0.1254) | 155.1 (0.2342) |

Table 2: ECP , WS and VS of different SCIs under the unit-level logistic model. Nominal coverage probability is 95%.

with random effects and numerical approximations inflates the variance. It is noteworthy that the modelling using the unit-level model is inferior than the Poisson modeling on several grounds. First of all, the simultaneous intervals are wider and they have poorer coverage. Secondly, the estimation of EBP on the basis of the sample at hand is more complex as it requires the creation of artificial categorical classes and the approximation of their true sizes. Already four covariates leads to $4^2 = 16$ categorical classes which significantly complicates the analysis. Last but not least, when we deal with a regular survey sample size (in our case more than 20000 units) the construction of intervals and estimation of MSE using a personal laptop takes up to 2 days, whereas in case of the area-level model from a few to several minutes (depending on the estimator of variability). The equivalents of Figure 1 and Figure 2 are deferred to Appendix D.4.

Above analysis on the area-level Poisson model and the empirical study on the unit-level binomial lead to following conclusions. First of all, the former model yields more accurate results already for small sample. Secondly, for the given sample size and data the ECP converges to the nominal level and it is not affected by the choice of the variability parameter. In addition, the distinction between SPCs and iCIs is crucial and the latter should not be employed in the simultaneous study. Finally, the numerical performance of our tests is satisfying. Given the simplicity of the SCI, iCI and tests based on $\sqrt{\hat{g}_{1d}}$ and its bootstrap equivalent, we restrict further presentations to them.

5 Predicting Poverty Rates in Galicia

Poverty estimation is of a great interest for statistical offices that have to provide reports as a basis on which local or central authorities decide about resource allocation and other polices to reduce poverty. Therefore, the interest is not in individual, randomly chosen small areas but in the total picture, and one has to provide SCI instead of iCI for the above discussed reasons. Specifically, we apply our methodology to provide SCIs for the estimates of the poverty levels, i.e., the proportions of inhabitants which live under the poverty line for each county of Galicia (applying the same poverty line to all counties). In our comparative analysis we estimate the poverty rates using the unit- and the area-level models described in Section 2.1 and 2.2. We make use of the general part of the Structural Survey for Homes in Galicia in 2015 with 23628 individuals within 9203 households located in 52 small areas. The survey does not produce official estimates at the domain level, but we managed to recover the direct estimators of the totals of

people being below the poverty line (Y_d), as well as the inhabitants of each county (N_d). In addition, under the area-level Poisson model we needed to calculate the number of units which fall into a particular category (X_{di}), e.g., number of employees or number of graduates in each county of Galicia, $i = 1, \dots, p$. The latter were used to obtain the covariates which are the proportions of individuals in each category $\bar{X}_{di} = X_{di}/N_d$. On the other hand, under the unit-level model, we needed to obtain the number of units N_{dl} falling into artificially created category z_{dl} , $d = 1, \dots, D$, $l = 1, \dots, L$ (see Section 2.2). The explicit formulas can be described as:

$$\begin{aligned} \hat{Y}_d^{dir} &= \sum_{j \in \mathcal{P}_d} w_{dj} y_{dj}, & \hat{N}_d^{dir} &= \sum_{j \in \mathcal{P}_d} w_{dj}, & \hat{N}_{dl}^{dir} &= \sum_{j \in \mathcal{P}_d} w_{dj} \mathbf{x}_{dj} \mathbb{1}_{\{\mathbf{x}_{dj} = \mathbf{z}_l\}}, \\ \hat{X}_{di}^{dir} &= \sum_{j \in \mathcal{P}_d} w_{dj} x_{dji}, & \text{and} & & \hat{\hat{X}}_{di}^{dir} &= \hat{X}_{di}^{dir} / \hat{N}_d^{dir}, \end{aligned} \quad (27)$$

where w_{dj} are sampling weights, and y_{dj} a binary variable with 1 indicating that an individual is below a poverty line. The poverty threshold is calculated from the survey being 0.6 of the median household income per capita in Galicia, i.e., we are not working with county specific poverty lines. The number of 'capita' in each household was calculated using the OECD modified scale (the same technique is used by Eurostat). The model based approach of this paper assumes that the estimates in (27) are known, non-random quantities, following López-Vizcaíno et al. (2015). The Structural Survey of Homes provided many possible auxiliary variables. Under the unit-level model these are the binary variables with 1 indicating that a person belongs to a particular category, whereas under area-level – the county proportions. We consider the following categorical variables:

- for labor status: children (ls0), employed (ls1), unemployed (ls2), inactive (ls3).
- for education: less than primary (ed0), primary (ed1), first and second level secondary (ed2), higher education (ed3).
- for the size of the municipality: less than 10 000 (sm1), 10 000-50 000 (sm2), more than 50 000 (sm3).
- for nationality: Spanish (n1), not Spanish (n2).
- for age: < 15 (age1), 15 – 24 (age2), 25 – 49 (age3), 50 – 64 (age4), >= 65 (age4).

As said, we are interested in $\bar{\mu}_d^{(\cdot)} := \mu_d^{(\cdot)}/N_d$ with (\cdot) standing for P or B in case of Poisson and binomial model respectively. Since the covariates in the categories sum up to one, we dropped the reference categories ls0, ed0, sm3, n1 and age1. Then we fitted the data to our area-, and the unit-level model of Hobza and Morales (2016). We retained only significant covariates with a p-value smaller than 0.05. Table 3 shows the remaining covariates with their estimated coefficients under area-level and unit-level models. In case of the former, the signs of the covariates are consistent with our expectations; unemployment and young age are associated with higher poverty rates, whereas higher level of studies or living in a small municipality is associated with lower poverty rates. The parameter estimate of the gamma distribution of the area effect is $\hat{\delta}^P = 2.48$. On the other hand, under the unit-model the signs of all covariates are positive, and $\hat{\delta}^B = 0.35$.

| Model | Area-level | | | | Unit-level | | | |
|-------------|------------|-------|------------|------------|------------|-------|------------|------------|
| Coefficient | Estimate | SE | z -value | $P(> z)$ | Estimate | SE | z -value | $P(> z)$ |
| Intercept | 10.038 | 0.669 | 15.005 | 0.000 | -2.048 | 0.067 | -30.415 | 0.000 |
| ls2 | 7.747 | 3.091 | 2.506 | 0.012 | 0.989 | 0.052 | 19.160 | 0.000 |
| ed2 | -3.136 | 1.201 | -2.611 | 0.009 | 0.172 | 0.039 | 4.442 | 0.000 |
| age2 | 11.317 | 4.023 | 2.813 | 0.005 | 0.760 | 0.058 | 13.033 | 0.000 |
| sm1 | -2.466 | 0.267 | -9.224 | 0.000 | 0.100 | 0.050 | 1.993 | 0.046 |

Table 3: Estimates of regression parameters under the area- and the unit-level model with $\hat{\delta}^P = 2.48$ and $\hat{\delta}^B = 0.35$, respectively.

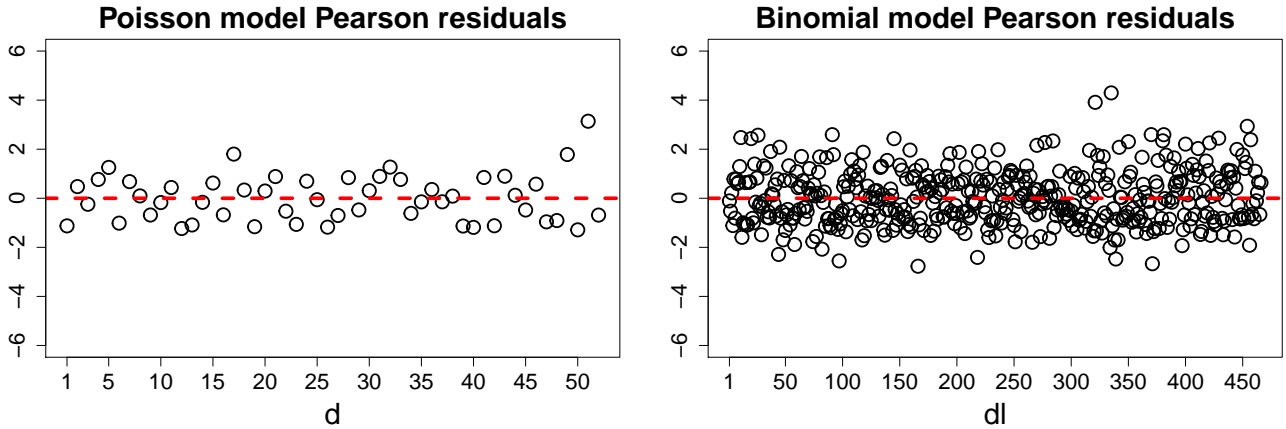


Figure 3: Diagnostic plots with Pearson residuals for: (left) the area-level model and (right) the unit-level model.

Figure 3 reports diagnostic plots with Pearson residuals for the area-level model in the left panel and for unit-level in the right panel. In case of the former, conditionally on random effects, y_d is distributed according to the negative binomial distribution (see Section 2.1 and the Pearson residuals were calculated for each county d). In contrast, under unit-level model we obtained them for each domain d and a covariate class l . Conditional distribution of y_{dl} is binomial with parameters (n_{dk}, p_{dk}) . The plots do not demonstrate any serious departures from normality that may indicate data misspecification.

Figure 4 shows point and iCI bootstrap estimates of proportions under Poisson and the binomial model. It is worth mentioning that in this plot we aim to compare the estimate $\hat{\mu}_d^{(l)}$, $d = 1, \dots, D$ within two modeling frameworks, not to compare estimates across different areas within the same model. Observe that for the majority of the areas, the point estimators are relatively close for both models. Yet, the difference between MSE estimates, and consequently between the lengths of the intervals, is the most striking feature of Figure 4. This does not change when switching to SCIs, see Figure 5. Again, the interval estimates under the unit-level model are much wider due to the much larger MSE estimates. The difference, though, is not only in the variability, but also in the bias. For example, in one case (sixth area in the third panel), the iCI estimates under both models do not even overlap.

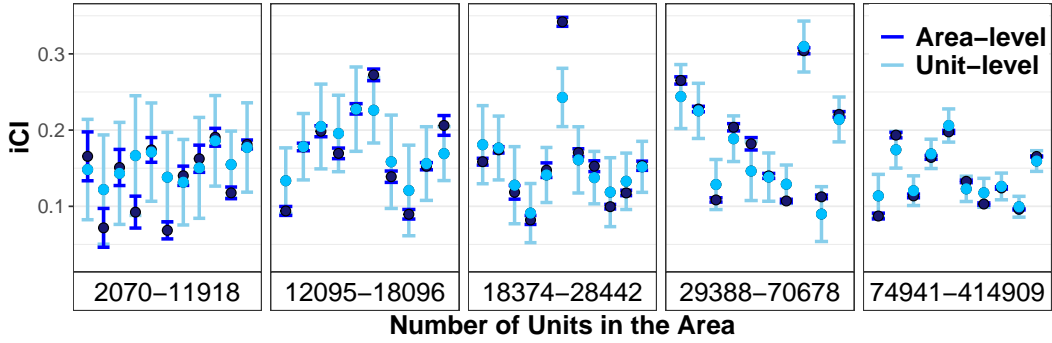


Figure 4: 95% iCI bootstrap estimates under area- and unit-level models.

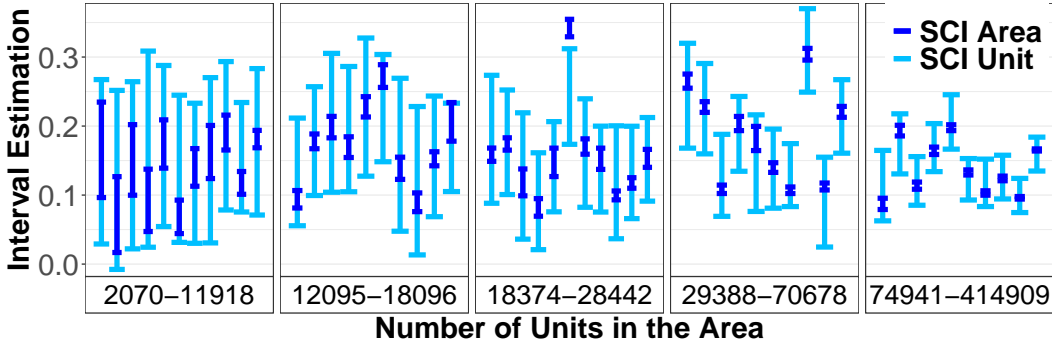


Figure 5: 95% SCI under area- and unit-level models.

Figure 6 presents bootstrap iCI and SCI constructed using $\hat{\sigma}(\hat{\zeta}_d) = \sqrt{\hat{g}_{1d}}$ defined in (10) and its bootstrap equivalent under the Poisson area-model. The picture for the unit-level logit model is given in Figure 7. Already our reliability study in Section 4 indicated that the unit-level model gives by far larger MSE estimates (cfr. Table 1 and 2). The high variability among the widths of iCIs (and SCIs respectively) is due to the different sample sizes. When comparing iCIs and SCIs, in many cases (e.g., first and the second county of the first panel in Figure 6) iCI would insinuate statistically different poverty levels, whereas SCI does not confirm this. Recall that for SCIs such multiple comparisons are valid, contrary to comparisons using iCIs. Recall that at least 5% of true poverty levels is not even contained in their iCIs.

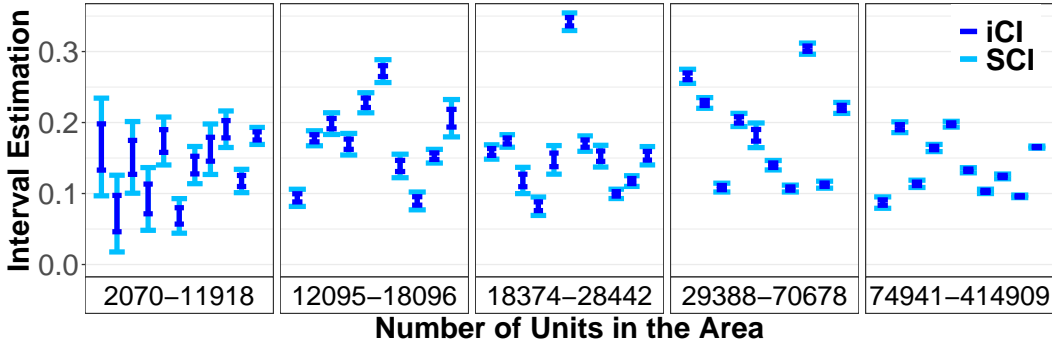


Figure 6: 95% iCI and bootstrap SCI estimates for EBP poverty rates in counties of Galicia under the area-level Poisson model.

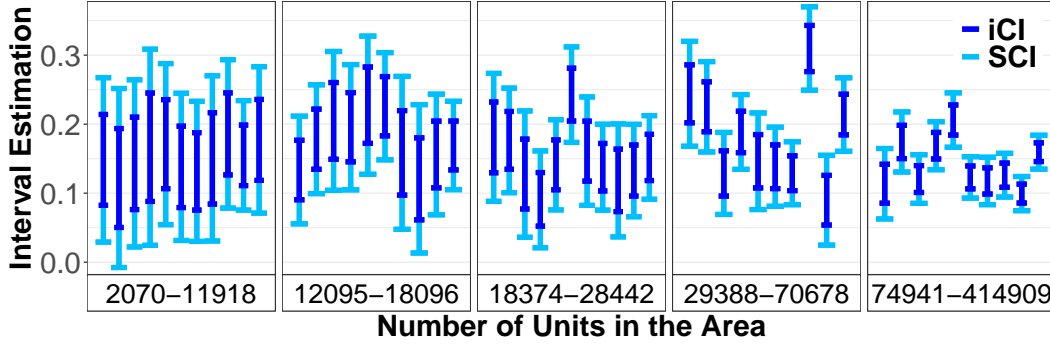


Figure 7: 95% iCI and bootstrap SCI for EBP poverty rates in counties of Galicia under the unit-level logit model.

Since the estimates under the area-level model are much less volatile, but according to our reliability study more reliable, we stick to this modeling framework for the rest of the section. Figure 8 depicts maps of the counties which present the lower and the upper boundary of the bootstrap SCIs. We observe a higher level of poverty in the interior and a south-western part of the region whereas a lower poverty level is typical for the northern part. Finally, we wish to

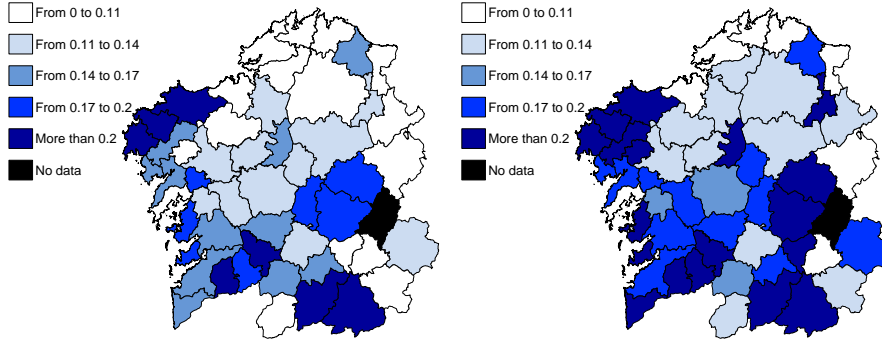


Figure 8: SCIs of EBP poverty proportions: (left) lower boundary, (right) upper boundary.

statistically investigate whether men and women are equally affected by poverty. Similarly as above, we want to test for equality on the county level across the entire Galicia. Observe that testing for each county individually at the $\alpha = 5\%$ error level results in rejection of at least 5% of the hypotheses of no difference in poverty levels. Therefore, we need to apply our max-type statistic in MTP introduced in Section 3. To test for equality between gender, we consider clusters created from the cross section of gender and county such that $\zeta \in \mathbb{R}^{104}$. We test $H_0 : \mathbf{B}\zeta = \mathbf{0}_{52}$ versus $H_1 : \mathbf{B}\zeta \neq \mathbf{0}_{52}$ where $\mathbf{B} \in \mathbb{R}^{52 \times 104}$ with rows being vectors with 1 on the $2d - 1$ place, -1 on $2d$ place, and 0 elsewhere. The max-type test statistic yields

$$t_H = \max_{d=1, \dots, D} \frac{|\mathbf{B}\hat{\zeta}|}{\hat{\sigma}(\hat{\zeta})} \approx 20.489,$$

while the bootstrap critical value under H_0 is $q_{BH_0}(1 - \alpha) \approx 2.999$. In conclusion, we clearly reject the hypothesis of no difference. Nevertheless, our test does not support the hypothesis that females are more affected than men, nor vice versa, see Figure 9.

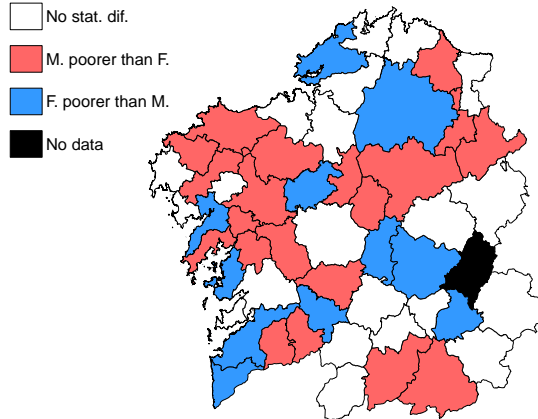


Figure 9: Simultaneous testing of no difference in poverty rates between women (F) and men (M).

6 Conclusions

We develop a methodology that allows for statistically valid simultaneous inference for EBP under GLMM. EBP is quite popular for poverty analysis in small areas. With a combination of our max-type statistics and consistent bootstrap estimators of its distribution we construct SCIs and MTPs. Our tools enable practitioners to make comparisons between all areas. This is particularly relevant for statistical offices and policy makers who decide about resource re-allocations. The multiple test is a valuable tool to make statistically valid joint conclusions about several or all areas. It is clear that the existing methods, i.e., iCIs, by construction are not suitable for such analyses and findings.

Moreover, we found two interesting features in our modeling approaches. Firstly, we introduce various bootstrap versions of statistics to construct SCIs and MPTs, which differ by the estimators of variability of $\hat{\sigma}(\hat{\zeta}_d)$. Interestingly, within our framework, the resulting statistics exhibit quite similar performances without indicating a clear winner. Our preference for \hat{g}_{1d} based methods is mainly due to their simplicity.

Secondly, our area-level Poisson modeling approach avoids complex integration. This does lead to tremendous computational gains (by a factor of 561). It makes the area-level model more attractive than its unit-level counterpart giving better prediction results in both, precision and efficiency. Furthermore, computation of EBP is much simpler and it does not require a construction of artificial covariate classes. Finally, our proposal is general enough to be extended straightforwardly to more complex data structures which for example account for a spatio-temporal correlations.

A Regularity conditions

In this section we state the regularity conditions.

1. $\hat{u}_d = \arg \max_{u_d \in \mathbb{R}} [\log g_d(\mathbf{y}_d | u_d, \boldsymbol{\theta}) + \log h(u_d)]$
2. $l(\boldsymbol{\theta})$ exists and is well-defined if:

R_1 . $l(\boldsymbol{\theta})$ is uniquely maximized and $\boldsymbol{\theta}_0 \in \Theta$.

R_2 . $l(\boldsymbol{\theta})$ is continuous.

R_3 . $l(\boldsymbol{\theta})$ and $\hat{l}(\boldsymbol{\theta})$ are concave.

R_4 . $\boldsymbol{\theta}_0$ is an interior point of the parameter space and the estimator $\hat{\boldsymbol{\theta}}$ is an interior point of the neighbourhood of $\boldsymbol{\theta}_0$ $\mathcal{N}_r(\boldsymbol{\theta}_0) = \{\boldsymbol{\theta} \mid \|\boldsymbol{\theta}_0 - \boldsymbol{\theta}\| < r\}$

R_5 . $\hat{l}(\boldsymbol{\theta})$ converges uniformly in probability to $l(\boldsymbol{\theta})$.

3. \mathbf{x}_{dj} are bounded and $\mathbb{E}(y_{dj}^m) < \infty$ for all $d \in [D]$, $j \in [n_d]$, where m is suitable large.
4. For each fixed \mathbf{y} , a score equation is continuously differentiable and $\mathbb{E}[S(\boldsymbol{\theta})] = 0$ if $\boldsymbol{\theta}$ is a true parameter value.
5. $\liminf_n \lambda[n^{-1}\text{Var}(s_n(\boldsymbol{\theta}))] > 0$ and $\liminf_n \lambda[-n^{-1}\mathbb{E}(\nabla s_n(\boldsymbol{\theta}))] > 0$ where $s_n(\boldsymbol{\theta}) = \sum_i^h \psi_i$, $\nabla s_n(\boldsymbol{\theta}) = \frac{\partial s_n(\boldsymbol{\theta})}{\partial \boldsymbol{\theta}}$ and $\lambda[A]$ indicates the smallest eigenvalue of matrix A .

The first two refer to log-likelihood function and they are necessary for the existence of the solution of maximum likelihood equations and $l(\boldsymbol{\theta})$ (see for example Bianconcini (2014)). On the other hand, conditions 3-5 are needed for the derivation of MSE estimators. Observe that these correspond to conditions in Jiang and Lahiri (2001).

B MSE of EBP under GLMM

Below we provide a decomposition of EBP under GLMM. Consider a general EBP $\hat{\zeta}_d$

$$\begin{aligned} \text{MSE}(\hat{\zeta}_d) &= \mathbb{E}[(\hat{\zeta}_d - \zeta_d)^2] = \mathbb{E}[(\hat{\zeta}_d - \tilde{\zeta}_d + \tilde{\zeta}_d - \zeta_d)^2] \\ &= \mathbb{E}[(\hat{\zeta}_d - \tilde{\zeta}_d)^2 + (\tilde{\zeta}_d - \zeta_d)^2 + 2\{(\hat{\zeta}_d - \tilde{\zeta}_d)(\tilde{\zeta}_d - \zeta_d)\}] \\ &= \mathbb{E}[(\hat{\zeta}_d - \tilde{\zeta}_d)^2] + \mathbb{E}[(\tilde{\zeta}_d - \zeta_d)^2] =: g_{2d} + g_{1d}, \end{aligned} \tag{28}$$

where the fourth equality follows by the law of iterated expectation, that is

$$\mathbb{E}[(\hat{\zeta}_d - \tilde{\zeta}_d)(\tilde{\zeta}_d - \zeta_d)] = \mathbb{E}\{(\hat{\zeta}_d - \tilde{\zeta}_d)\mathbb{E}[(\tilde{\zeta}_d - \zeta_d)|\mathbf{y}_d]\} = 0,$$

by the definition of $\tilde{\zeta}_d(\boldsymbol{\theta}) = \mathbb{E}[\zeta_d|\mathbf{y}_d]$. Furthermore, we can decompose g_{1d} to obtain

$$g_{1d} = \mathbb{E}[(\tilde{\zeta}_d - \zeta_d)^2] = \mathbb{E}(\tilde{\zeta}_d^2) + \mathbb{E}(\zeta_d^2) - 2\mathbb{E}[\tilde{\zeta}_d\mathbb{E}(\zeta_d|\mathbf{y}_d)] = \mathbb{E}(\zeta_d^2) - \mathbb{E}(\tilde{\zeta}_d^2) \tag{29}$$

once again by the definition of $\tilde{\zeta}_d$.

C Area-level Poisson model

C.1 Estimation of parameters

As far as the estimation method of $\boldsymbol{\theta}$ is taken into account, we followed the suggestion of Lawless (1987) and we implemented Newton-Raphson and Fisher scoring algorithms. Application of both

methods leads to a following iterative scheme

$$\boldsymbol{\theta}^{(i+1)} = \boldsymbol{\theta}^{(i)} - \mathbf{H}_P^{-1}(\boldsymbol{\theta}^{(i)})\mathbf{s}_P(\boldsymbol{\theta}^{(i)}), \quad (30)$$

where $\mathbf{s}_P(\boldsymbol{\theta})$ is a score vector composed of the first derivative of the likelihood and $\mathbf{H}_P^{-1}(\boldsymbol{\theta})$ stands for the observed information matrix $\mathbf{J}_P(\boldsymbol{\theta}) = -\mathbf{H}_P^{-1}(\boldsymbol{\theta})$ under a Newton-Raphson and an information matrix $\mathbf{I}_P(\boldsymbol{\theta}) = \mathbb{E}[\mathbf{J}_P(\boldsymbol{\theta})]$ under Fisher scoring. Let a score vector $\mathbf{s}_P(\boldsymbol{\theta})$ be defined as $\mathbf{s}_P(\boldsymbol{\theta}) = (s_{P1}(\boldsymbol{\theta}), s_{P2}(\boldsymbol{\theta}), \dots, s_{Pp+1}(\boldsymbol{\theta}))^t$. Its components are given as follows

$$s_{Pk} = \frac{\partial l^P}{\partial \beta_k} = \sum_{d=1}^D \frac{x_{dk}(y_d - \lambda_d)}{1 + \alpha \lambda_d}, \quad , k = 1, 2, \dots, p,$$

$$s_{Pk+1} = \frac{\partial l^P}{\partial \alpha} = \sum_{d=1}^D \left[\sum_{j=1}^{y_d-1} \left(\frac{j}{1 + \alpha j} \right) + \alpha^{-2} \log(1 + \alpha \lambda_d) - \frac{(y_d + \alpha^{-1})\lambda_d}{1 + \alpha \lambda_d} \right],$$

with $\alpha = \delta^{-1}$. The observed information matrix is composed of the negative second derivatives of the likelihood, that is

$$\mathbf{J}_{Pkr} = -\frac{\partial^2 l^P}{\partial \beta_k \partial \beta_r} = \sum_{d=1}^D \frac{(1 + \alpha y_d)\lambda_d x_{dr} x_{dk}}{(1 + \alpha \lambda_d)^2}, \quad k, r = 1, \dots, p,$$

$$\mathbf{J}_{Pk(r+1)} = -\frac{\partial^2 l^P}{\partial \beta_k \partial \alpha} = \sum_{d=1}^D \frac{\lambda_d (y_d - \lambda_d) x_{dr}}{(1 + \alpha \lambda_d)^2}, \quad k = 1, \dots, p,$$

$$\mathbf{J}_{P(k+1)(r+1)} = -\frac{\partial^2 l^P}{\partial^2 \alpha} = \sum_{d=1}^D \left[\sum_{j=1}^{y_d-1} \left(\frac{j}{1 + \alpha j} \right)^2 + 2\alpha^{-3} \log(1 + \alpha \lambda_d) - \frac{2\alpha^{-2}\lambda_d}{1 + \alpha \lambda_d} - \frac{(y_d + \alpha^{-1})\lambda_d^2}{(1 + \alpha \lambda_d)^2} \right].$$

On the other hand, the Fisher information matrix, which is assured to be positive definite, is composed of

$$\mathbf{I}_{Pkr} = \sum_{d=1}^D \frac{\lambda_d x_{dr} x_{dk}}{(1 + \alpha \lambda_d)}, \quad k, r = 1, \dots, p,$$

$$\mathbf{I}_{Pk(r+1)} = 0, \quad k = 1, \dots, p,$$

$$\mathbf{I}_{P(k+1)(r+1)} = \alpha^{-4} \sum_{d=1}^D \left[\mathbb{E} \sum_{j=1}^{y_d-1} (\alpha^{-1} + j)^{-2} - \frac{\alpha \lambda_d}{\lambda_d + \alpha^{-1}} \right].$$

The details of this derivation and some suggestions regarding the calculation are in Lawless (1987). It is necessary to point out that we followed one of them and first we maximized $l(\boldsymbol{\theta})$ with respect to fixed parameters for selected values of α using Newton Raphson and the Fisher scoring. In this way we obtained the profile likelihood $l(\tilde{\boldsymbol{\theta}}(\alpha), \alpha)$. Since the Fisher scoring algorithm was numerically more stable, Section C.4 contains the results obtained using this algorithm. We follow the suggestion of Boubeta et al. (2016) when it comes to the choice the starting values, namely we set $\boldsymbol{\beta}^{(0)} = \tilde{\boldsymbol{\beta}}$, where $\tilde{\boldsymbol{\beta}}$ is the maximum likelihood estimator under the model without the random effects. When it comes to α , we use the properties of a random variable which is distributed

according to negative binomial, that is $\sigma_d^2 := \text{Var}(y_d) = \lambda_d + \alpha\lambda_d^2$. Therefore σ_d^2 can be estimated applying

$$\tilde{\sigma}_d^2 = \frac{1}{D} \sum_{d=1}^D (\mathbf{x}_d^t \tilde{\boldsymbol{\beta}} - \log y_d)^2 \quad \text{and} \quad \alpha^{(0)} = \frac{\tilde{\sigma}_d^2 - \mathbf{x}_d^t \tilde{\boldsymbol{\beta}}}{(\mathbf{x}_d^t \tilde{\boldsymbol{\beta}})^2}.$$

C.2 Estimation of MSE of EBP

Let us turn to the derivation of MSE for EBP $\hat{\mu}^P$ for which BP is defined as

$$\mathbb{E}(\mu_d^P | y_d) = \frac{\int_0^\infty \lambda_d w_d g(y_d | w_d) h(w_d) dw_d}{\int_0^\infty g(y_d | w_d) h(w_d) dw_d} = \frac{A_d^P(y_d, \boldsymbol{\theta})}{C_d^P(y_d, \boldsymbol{\theta})} = \frac{\lambda_d(y_d + \delta)}{(\lambda_d + \delta)} =: \psi_d^P(y_d, \boldsymbol{\theta}). \quad (31)$$

Firstly, we focus on $\mathbb{E}(\zeta_d^2)$ from (29)

$$\begin{aligned} \kappa_{1d} := \mathbb{E}[\mu_d^{P2}] &= \int_0^\infty \lambda_d^2 w_d^2 f(w_d) dw_d = \int_0^\infty \lambda_d^2 w_d^2 \frac{\delta^\delta \exp(-w_d \delta) w_d^{\delta-1}}{\Gamma(\delta)} dw_d \\ &= \frac{\lambda_d^2 \delta^\delta \Gamma(\delta + 2)}{\Gamma(\delta) \delta^{\delta+2}} \int_0^\infty \frac{\delta^{\delta+2} \exp(-w_d \delta) w_d^{\delta+2-1}}{\Gamma(\delta + 2)} dw_d = \frac{\lambda_d^2 (\delta + 1)}{\delta} \end{aligned}$$

and $\mathbb{E}(\tilde{\zeta}_d^2)$ under area-level Poisson model is

$$\kappa_{2d} := \mathbb{E}[\tilde{\mu}_d^{P2}] = \mathbb{E}[\mathbb{E}^2(\mu_d^P | y_d)] = \mathbb{E}[\psi_d^{P2}(y_d, \boldsymbol{\theta})] = \mathbb{E} \left[\frac{\lambda_d^2 (y_d + \delta)^2}{(\lambda_d + \delta)^2} \right] = \sum_{j=0}^\infty \frac{\lambda_d^2 (j + \delta)^2}{(\lambda_d + \delta)^2} P(y_d = j),$$

where we used (31) to obtain a final expression. When it comes to the estimation of g_{2d} in (28) under Poisson area-level model, we use Taylor expansion, that is

$$\begin{aligned} \hat{\mu}_d^P - \tilde{\mu}_d^P &= \psi_d(y_d, \hat{\boldsymbol{\theta}}) - \psi_d(y_d, \boldsymbol{\theta}) \\ &= \left(\frac{\partial}{\partial \boldsymbol{\theta}} \psi_d(y_d, \boldsymbol{\theta}) \right)^t (\hat{\boldsymbol{\theta}} - \boldsymbol{\theta}) + \frac{1}{2} (\hat{\boldsymbol{\theta}} - \boldsymbol{\theta})^t \left(\frac{\partial^2}{\partial \boldsymbol{\theta}^2} \psi_d(y_d, \boldsymbol{\theta}) \right) (\hat{\boldsymbol{\theta}} - \boldsymbol{\theta}) + o(\|\hat{\boldsymbol{\theta}} - \boldsymbol{\theta}\|^2). \end{aligned} \quad (32)$$

In addition, we assume standard regularity conditions for ML estimators from Appendix in the main document and we have $\|\hat{\boldsymbol{\theta}} - \boldsymbol{\theta}\| = O_P(n^{-1/2})$. Hence, it follows

$$\mathbb{E} \left[(\hat{\mu}_d^P(\hat{\boldsymbol{\theta}}) - \tilde{\mu}_d^P(\boldsymbol{\theta}))^2 \right] = \frac{1}{D} \mathbb{E} \left[\left(\left(\frac{\partial}{\partial \boldsymbol{\theta}} \psi_d(y_d, \boldsymbol{\theta}) \right)^t \sqrt{D} (\hat{\boldsymbol{\theta}} - \boldsymbol{\theta}) \right)^2 \right] + o(1/D). \quad (33)$$

Now we apply to ML estimator the construction of Jiang and Lahiri (2001). We define an estimator $\hat{\boldsymbol{\theta}}_{d-}$ based on $\mathbf{y}_{d-} = (y_1, \dots, y_{d-1}, y_d, \dots, y_D)$ and $\hat{\mu}_{d-}^P = \psi_d(y_d, \hat{\boldsymbol{\theta}}_{d-})$ and we replace $\hat{\boldsymbol{\theta}}$ (33) with $\hat{\boldsymbol{\theta}}_{d-}$.

Then

$$\begin{aligned}
c_{-d}(\boldsymbol{\theta}) &= \mathbb{E} \left[\left(\left(\frac{\partial}{\partial \boldsymbol{\theta}} \psi_d(y_d, \boldsymbol{\theta}) \right)^t \sqrt{D} (\hat{\boldsymbol{\theta}}_{d-} - \boldsymbol{\theta}) \right)^2 \right] \\
&= \sum_{j=1}^{\infty} \mathbb{E} \left[\left(\left(\frac{\partial}{\partial \boldsymbol{\theta}} \psi_d(y_d, \boldsymbol{\theta}) \right)^t \sqrt{D} (\hat{\boldsymbol{\theta}}_{d-} - \boldsymbol{\theta}) \right)^2 \Big|_{y_d=j} \right] P(y_d = j) \\
&= \sum_{j=1}^{\infty} \left(\frac{\partial}{\partial \boldsymbol{\theta}} \psi_d(y_d, \boldsymbol{\theta}) \right)^t \mathbb{V}ar_{-d}(\boldsymbol{\theta}) \left(\frac{\partial}{\partial \boldsymbol{\theta}} \psi_d(y_d, \boldsymbol{\theta}) \right) P(y_d = j)
\end{aligned} \tag{34}$$

where $\mathbb{V}ar_{-d}(\boldsymbol{\theta}) = D \mathbb{E} \left[(\hat{\boldsymbol{\theta}}_{d-} - \boldsymbol{\theta}) (\hat{\boldsymbol{\theta}}_{d-} - \boldsymbol{\theta})^t \right]$ which does not depend on the value of y_d . Therefore

$$\text{MSE}(\hat{\mu}_{-d}^P) = g_{1d}(\boldsymbol{\theta}) + \frac{1}{D} c_{-d}(\boldsymbol{\theta}) + o(1/D)$$

Furthermore, if we suppose that conditions 1-2 from Appendix hold, plug-in MSE is given as follows

$$\text{MSE}(\hat{\mu}_d^P) = \kappa_{1d}(\boldsymbol{\theta}) - \kappa_{2d}(\boldsymbol{\theta}) + \frac{1}{D} c_d(\boldsymbol{\theta}) + o(1/D) \tag{35}$$

with c_d defined as above replacing $\hat{\boldsymbol{\theta}}_{d-}$ and $\mathbb{V}ar_{-d}$ by $\hat{\boldsymbol{\theta}}_d$ and $\mathbb{V}ar_d$.

C.3 Consistency of SCI

We assume a general EBP ζ_d . The proofs follows within the same lines as in Chatterjee et al. (2008) and Reluga et al. (2019). Let $g_d := g_d(\boldsymbol{\theta})$ and $\hat{g}_d := \hat{g}_d(\hat{\boldsymbol{\theta}})$ and we look at the properties of $G_d(w)$.

$$\begin{aligned}
G_d(w) &= \mathbb{P} \left(\frac{\hat{\zeta}_d - \zeta_d}{\sqrt{g_d}} \leq w \right) = \mathbb{E} \left\{ P \left(\frac{\tilde{\zeta}_d - \zeta_d}{\sqrt{g_d}} \leq w + \left[\frac{w(\sqrt{\hat{g}_d} - \sqrt{g_d}) + \hat{\zeta}_d - \tilde{\zeta}_d}{\sqrt{g_d}} \right] \right) \Big| \mathbf{y}_d \right\} \\
&= \mathbb{E} \{ \Phi[w + Q(w, \mathbf{y}_d)] \} \\
&= \Phi(w) + \phi(w) \mathbb{E} [Q(w, \mathbf{y}_d)] - 2^{-1} w \phi(w) \mathbb{E} [Q^2(w, \mathbf{y}_d)] \\
&\quad + 2^{-1} \mathbb{E} \left\{ \int_w^{w+Q(w, \mathbf{y}_d)} (w + Q(w, \mathbf{y}_d) - x)^2 (x^2 - 1) \phi(x) dx \right\}.
\end{aligned}$$

Using some classical results and a triangle inequality it follows immediately that the last term is bounded by $\mathbb{E}|Q|^3$ and it is of smaller order than the first three terms. Therefore the first step towards consistency of SCIs is to quantify the asymptotic expansions of $\mathbb{E}[Q(w, \mathbf{y}_d)]$ and $\mathbb{E}[Q^2(w, \mathbf{y}_d)]$. We decompose $Q(w, \mathbf{y}_d)$ into

$$Q(w, \mathbf{y}_d) = \frac{\hat{\zeta}_d - \tilde{\zeta}_d}{\sqrt{g_d}} + \frac{w(\sqrt{\hat{g}_d} - \sqrt{g_d})}{\sqrt{g_d}} = Q_1 + Q_2.$$

From now on we focus on the area-level model only. Under different models the calculations would be equivalent. As for Q_1 , it has been found in (32) that

$$\hat{\mu}_d^P - \tilde{\mu}_d^P = \left(\frac{\partial}{\partial \boldsymbol{\theta}} \psi_d(y_d, \boldsymbol{\theta}) \right)^t (\hat{\boldsymbol{\theta}} - \boldsymbol{\theta}) + o\left(\frac{1}{\sqrt{D}}\right)$$

as well as

$$\begin{aligned} \mathbb{E}(\hat{\mu}_d^P - \tilde{\mu}_d^P) &= \frac{1}{\sqrt{D}} \mathbb{E} \left[\left(\frac{\partial}{\partial \boldsymbol{\theta}} \psi_d(y_d, \boldsymbol{\theta}) \right)^t \sqrt{D} (\hat{\boldsymbol{\theta}} - \boldsymbol{\theta}) \right] + o\left(\frac{1}{\sqrt{D}}\right) \quad \text{and} \\ \mathbb{E} [(\hat{\mu}_d^P - \tilde{\mu}_d^P)^2] &= O(D^{-1}), \end{aligned}$$

where the second equality is due to (33). Furthermore, we recall that $g_d = \kappa_{1d} + \kappa_{2d}$, i.e., the first term is unknown constant. Moreover, since a negative binomial r.v. has a finite second moment, the second term κ_{2d} is an infinitive series which converges to some constant. Thus the square root of g_d is a constant too and that results in $\mathbb{E}(Q_1) = O(D^{-1/2})$ as well as $\mathbb{E}(Q_1^2) = O(D^{-1})$.

If we now turn to Q_2 , we have an immediate simplification

$$Q_2 = \frac{w(\sqrt{\hat{g}_d} - \sqrt{g_d})}{\sqrt{g_d}} = w \left(\sqrt{\frac{\hat{g}_d}{g_d}} - 1 \right).$$

Similarly to the computations above and following Boubeta et al. (2016), we can use a Taylor expansion for \hat{g}

$$\hat{g}_d(\hat{\boldsymbol{\theta}}) = g_d(\boldsymbol{\theta}) + \left(\frac{\partial}{\partial \boldsymbol{\theta}} g_d(\boldsymbol{\theta}) \right)^t (\hat{\boldsymbol{\theta}} - \boldsymbol{\theta}) + \frac{1}{2} (\hat{\boldsymbol{\theta}} - \boldsymbol{\theta})^t \left(\frac{\partial^2}{\partial^2 \boldsymbol{\theta}} g_d(\boldsymbol{\theta}) \right) (\hat{\boldsymbol{\theta}} - \boldsymbol{\theta}) + o(\|\hat{\boldsymbol{\theta}} - \boldsymbol{\theta}\|^2).$$

Therefore we have

$$\mathbb{E}[\hat{g}_d(\hat{\boldsymbol{\theta}})] = g_d(\boldsymbol{\theta}) + \left(\frac{\partial}{\partial \boldsymbol{\theta}} g_d(\boldsymbol{\theta}) \right)^t D \mathbb{E} [(\hat{\boldsymbol{\theta}} - \boldsymbol{\theta})] + O(D^{-1}).$$

Thus it follows that $\mathbb{E}(\sqrt{\hat{g}/g}) = O(D^{-1/2})$ and $\mathbb{E}(Q_2) = O(D^{-1/2})$ as well as $\mathbb{E}(Q_2^2) = O(D^{-1})$. Finally we deduce that under the area-level Poisson model $G_d(w)$ attains a short asymptotic expansion

$$G_d(w) = \Phi(w) + D^{-1/2} \gamma(w, \boldsymbol{\theta}) + O(D^{-1}).$$

A similar expansion can be established for $G_d^*(w)$ (defined in the main document) if we replace $\boldsymbol{\theta}$ with $\hat{\boldsymbol{\theta}}$.

C.4 Finite sample performance

As we have mentioned in the main document, for the performance study of the fixed effects $\boldsymbol{\beta}$ and variability parameter δ we used RBIAS and RRMSE which are defined as follows

$$RBIAS(\hat{\theta}_j) = \frac{1}{K} \sum_{k=1}^K (\hat{\theta}_j^{(k)} - \theta_j) / |\theta_j|, \quad RRMSE(\hat{\theta}_j) = \left(\sqrt{\frac{1}{K} \sum_{k=1}^K (\hat{\theta}_j^{(k)} - \theta_j)^2} \right) / |\theta_j|$$

where K is the number of simulations and $\theta_j \in \boldsymbol{\theta} = (\boldsymbol{\beta}, \delta)$, $j = 1, \dots, 6$. The empirical performance of the EBP $\hat{\zeta}_d$ is evaluated using bias (B_d), average absolute bias (B), MSE (E_d) and average MSE (E)

$$B_d = \frac{1}{K} \sum_{k=1}^K (\hat{\zeta}_d^{(k)} - \zeta_d^{(k)}), \quad B = \sum_{d=1}^D |B_d|/D, \quad E_d = \frac{1}{K} \sum_{k=1}^K (\hat{\zeta}_d^{(k)} - \zeta_d^{(k)})^2, \quad E = \sum_{d=1}^D |E_d|/D.$$

We have also calculated relative root MSE and the relative bias using slightly modified formulas for fixed parameters, that is

$$RBIAS(\hat{\zeta}_d^{(k)}) = B_d/\bar{\zeta}_d^{(k)}, \quad RRMSE(\hat{\zeta}_d^{(k)}) = \sqrt{E_d}/\bar{\zeta}_d^{(k)} \quad \text{where} \quad \bar{\zeta}_d^{(k)} = \frac{1}{K} \sum_{k=1}^K \zeta_d^{(k)}.$$

A detailed setting of the simulation study under area-level Poisson model is given in the main document. Table 4 outlines RBIAS and RRMSE of $\hat{\boldsymbol{\theta}}$. It is apparent that both criteria decrease with the growing sample size. Furthermore, Table 5 summarizes bias and MSE of EBP $\hat{\mu}_d^P$,

| D | $\hat{\beta}_0$ | $\hat{\beta}_1$ | $\hat{\beta}_2$ | $\hat{\beta}_3$ | $\hat{\beta}_4$ | $\hat{\delta}$ |
|----|------------------|------------------|------------------|------------------|------------------|-----------------|
| 26 | 0.0018 (0.1007) | -0.1006 (0.7333) | -0.0235 (0.5965) | -0.0519 (0.5710) | -0.0187 (0.1596) | 0.5364 (0.6934) |
| 52 | -0.0026 (0.0691) | -0.0201 (0.4043) | -0.0339 (0.4110) | -0.0337 (0.3561) | 0.0001 (0.1053) | 0.1540 (0.2758) |
| 78 | -0.0043 (0.0551) | -0.0004 (0.3330) | -0.0193 (0.3440) | 0.0035 (0.2897) | 0.0018 (0.0902) | 0.0887 (0.2043) |

Table 4: RBIAS and RRMSE (in parenthesis) for ML estimators under area-level Poisson model.

$d = 1, \dots, D$ for quantiles of the set $\{1, \dots, D\}$ where the domains are sorted by the sample size. The first column shows the average absolute biases and the average MSEs. The results confirm very good performance of this estimator. On the other hand, Figure 10 depicts RBIAS

| D | d | $B_d(E_d)$ | D | d | $B_d(E_d)$ | D | d | $B_d(E_d)$ |
|--------|----|------------------|--------|----|------------------|--------|----|------------------|
| 26 | 6 | -0.0001 (0.0000) | 52 | 11 | -0.0002 (0.0000) | 78 | 16 | -0.0003 (0.0000) |
| | 11 | -0.0001 (0.0000) | | 21 | -0.0001 (0.0000) | | 32 | -0.0001 (0.0001) |
| | 16 | 0.0001 (0.0000) | | 32 | 0.0000 (0.0001) | | 47 | 0.0000 (0.0001) |
| | 21 | 0.0001 (0.0001) | | 42 | 0.0002 (0.0002) | | 63 | 0.0002 (0.0003) |
| $B(E)$ | | 0.0002 (0.0001) | $B(E)$ | | 0.0003 (0.0001) | $B(E)$ | | 0.0003 (0.0002) |

Table 5: B_d , E_d and their averages B and E for the estimators of $\hat{\mu}_d$ under area-level Poisson model.

and RRMSE of $\hat{\zeta}_d^{(k)}$ under different sample sizes. The most striking feature, already mentioned in the main document, is an outstanding performance for $D = 26$ and poorer results for $D = 52$ and $D = 78$. Recall that the smallest sample was obtained by a simple random sampling from the pool of true areas. Relatively better performance can be thus explained by the fact that a couple of problematic areas were not selected. Extreme values are the most challenging to estimate – we found out that $D = 26$ was randomly truncated, because it does not include 3 lowest and 2 highest counts of people below poverty level (see histograms and box plot in Figure 13). As

a consequence, model was easier to fit and the EBP was estimated more accurately. Regarding $D = 52$ and $D = 72$, their performances are similar with lower median and more outliers for the highest sample size.

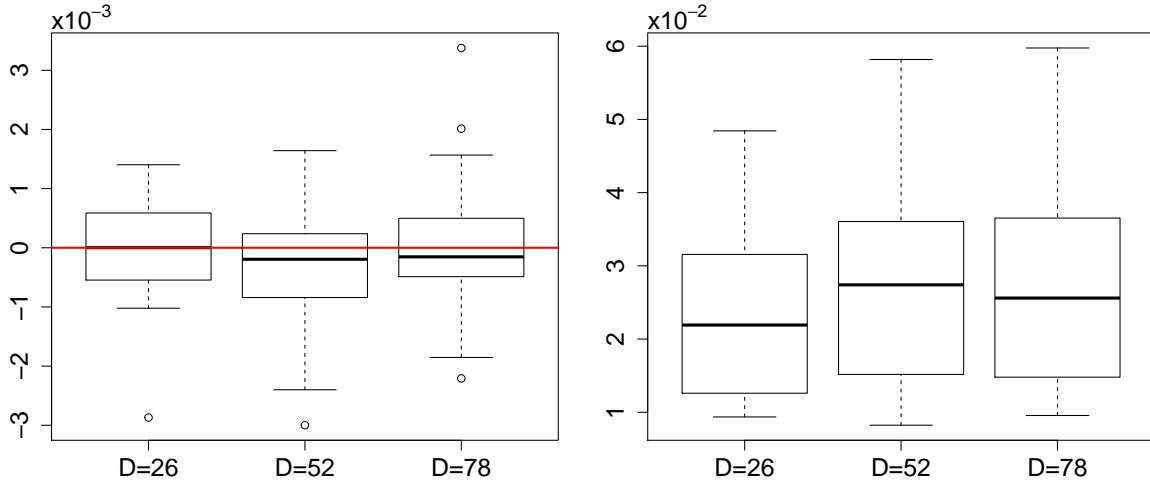


Figure 10: Box plots with (left) RBIAS and (right) RRMSE for $\hat{\zeta}_d^{(k)}$ under the area-level model.

Figure 11 and Figure 12 illustrate the performance of MSE and \hat{g}_{1d} respectively for each cluster $d = 1, \dots, D$. They are sorted in decreasing order. As far as MSE is concerned, the results are similar for bootstrap, bias corrected bootstrap and plug-in estimators. For $D = 26$, they are almost identical with the true value of MSE while for $D = 52$ and $D = 78$ they deviate slightly from truth for the highest values and become almost indistinguishable for the lowest values which is motivated by the same reasoning as Figure 10.

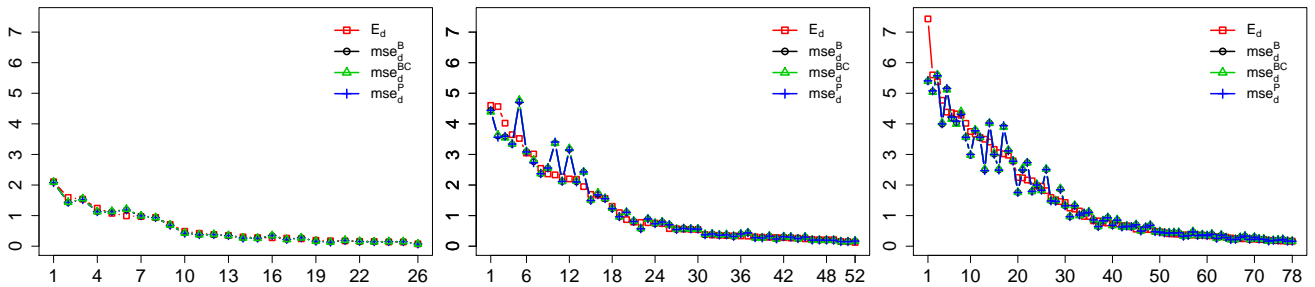


Figure 11: MSE estimators ($\times 10^4$): (left) $D = 26$, (centre) $D = 52$ and (right) $D = 78$ under area-level Poisson model.

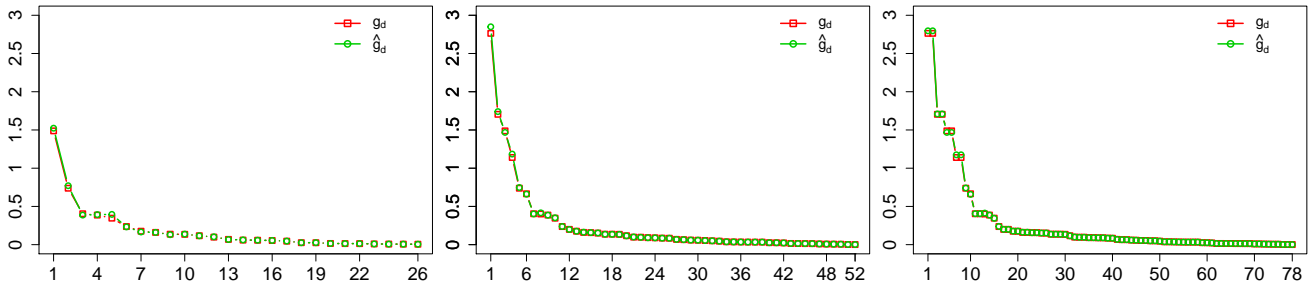


Figure 12: g_{1d} estimators ($\times 10^4$): (left) $D = 26$, (centre) $D = 52$ and (right) $D = 78$ under area-level Poisson model.

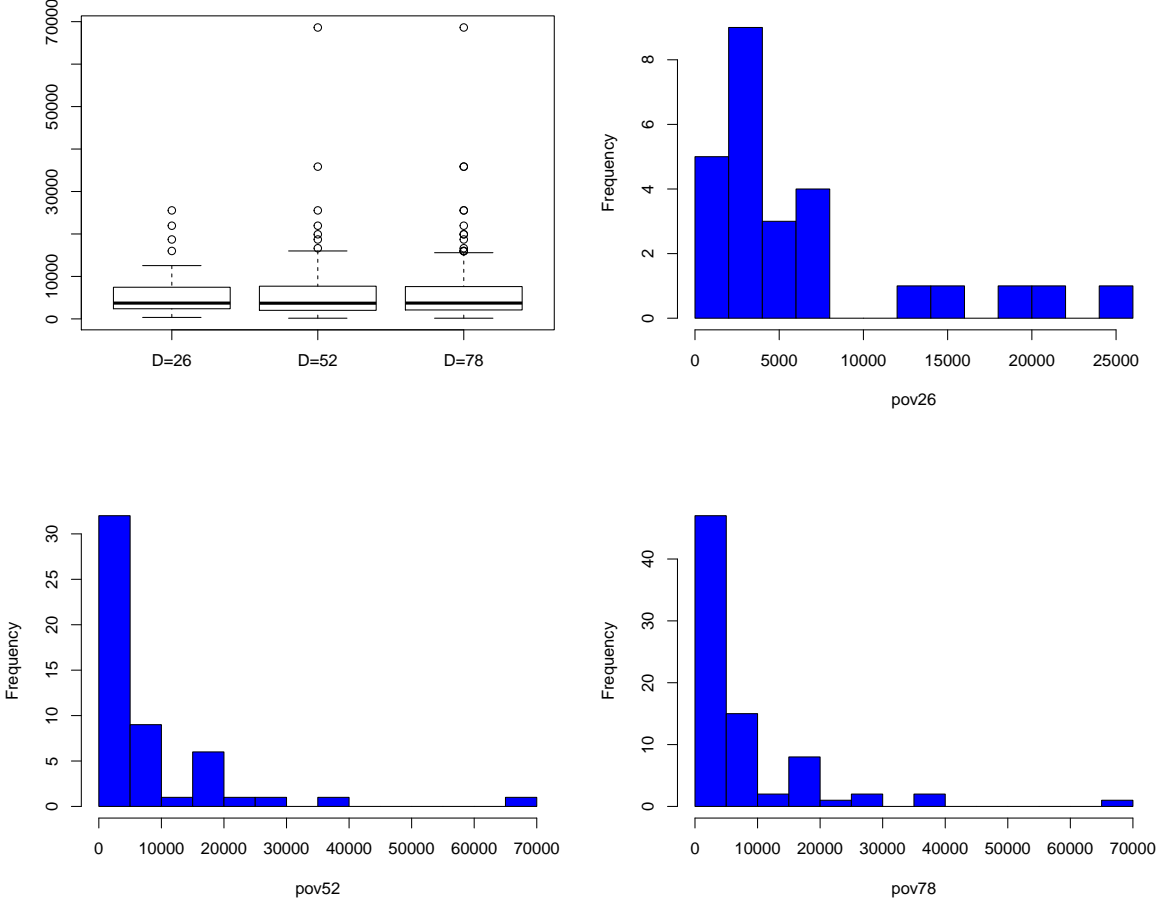


Figure 13: Box plot and histograms of response variable for $D = 26$, $D = 52$ and $D = 78$.

D Unit-level logit model

D.1 Estimation of the parameters

The unit-level binomial model is widely applied for counts or binary responses and it has been comprehensively discussed by, e.g., Hobza and Morales (2016). We propose a different estimation method, since almost all theoretical assumptions are more or less identical to those proposed by the authors we try to be as concise as possible not to hamper readability of the results.

There exist many methods to estimate the vector of model parameters $\boldsymbol{\theta}$. A direct maximization of the log-likelihood cannot be easily performed due to the presence of an integral in the log-likelihood function. Nevertheless, one can approximate the integral using AGQ or approximate the integrand applying Laplace approximation. We proceed with the former as it can be seen as a higher order version of the latter, i.e., it provides much smaller approximation error (Bianconcini, 2014). AGQ has been extremely popular and implemented by, e.g., Rabe-Hesketh et al. (2005) and Joe (2008). The second idea is to use the method of simulated moments suggested by Jiang (1998b) which was employed explicitly to estimate model parameter under unit-level logit and area-level Poisson models respectively by Hobza and Morales (2016) and Boubeta et al. (2016). In what follows, we proceed with the likelihood based methods which might be treated as a comparative study to the two aforementioned. Since our derivation follows tightly the theory developed by Bianconcini (2014) under generalized linear latent variable model (GLLVM), with some notational changes, but otherwise almost identical, we provide only the most important points.

Consider a GLMM with one dimensional normally distributed random effect. In this case, the structure of the exponential family allows us to write the likelihood contribution from each area d in a simplified form defining functions l_d

$$i_d(\boldsymbol{\theta}, u_d) = \sum_{j=1}^{n_d} \left[\frac{y_{dj} \gamma_{dj} - b(\gamma_{dj})}{\varphi} + c(y_{dj}, \varphi) \right] - \frac{1}{2} u_d^2.$$

Contributions from each area are conditionally independent. Therefore, the marginal distribution of the whole data vector under the exponential family is given as

$$\mathcal{L}(\boldsymbol{\theta}) := f(\mathbf{y}|\boldsymbol{\theta}) = \prod_{d=1}^D f_d(\mathbf{y}_d|\boldsymbol{\theta}) = (2\pi)^{-D/2} \prod_{d=1}^D \int_{\mathbb{R}} \exp [i_d(\boldsymbol{\theta}, u_d)] du_d.$$

The log-likelihood is then given as

$$l(\boldsymbol{\theta}) = -\frac{D}{2} \log(2\pi) + \sum_{d=1}^D \log \int_{\mathbb{R}} \exp [i_d(\boldsymbol{\theta}, u_d)] du_d. \quad (36)$$

The asymptotic properties of AGQ were studied by Bianconcini (2014) under generalized linear latent variable models (GLLVM). Due to the close similarity between both models, we can use her

results with a slightly different notation. Under GLMM a score equation is given by

$$\begin{aligned} \mathcal{S}(\boldsymbol{\theta}) &= \sum_{d=1}^D \frac{\partial \log f_d(\mathbf{y}_d|\boldsymbol{\theta})}{\partial \boldsymbol{\theta}} = \sum_{d=1}^D \frac{1}{f_d(\mathbf{y}_d|\boldsymbol{\theta})} \int_{\mathbb{R}} \frac{\partial}{\partial \boldsymbol{\theta}} [g_d(\mathbf{y}_d|u_d, \boldsymbol{\theta})h(u_d)] du_d \\ &= \sum_{d=1}^D \int_{\mathbb{R}} \mathcal{S}_d(\boldsymbol{\theta}; u_d)h(u_d|\mathbf{y}_d; \boldsymbol{\theta})du_d = \sum_{d=1}^D \mathbb{E}_{\mathbf{u}|\mathbf{y}} [\mathcal{S}_d(\boldsymbol{\theta}; u_d)] \end{aligned} \quad (37)$$

where $\mathcal{S}_d(\boldsymbol{\theta}; u_d)$ denotes $\partial \log f_d(\mathbf{y}_d|\boldsymbol{\theta})/\partial \boldsymbol{\theta} = \partial[\log g_d(\mathbf{y}_d|u_d, \boldsymbol{\theta}) + \log h(u_d)]/\partial \boldsymbol{\theta}$. The application of the AGQ requires rewriting an equation for a conditional likelihood under a specific form

$$f_d(\mathbf{y}_d|\boldsymbol{\theta}) = \int_{\mathbb{R}} \frac{g_d(\mathbf{y}_d|u_d, \boldsymbol{\theta})h(u_d)h_1(u_d|\hat{u}_d, \hat{\delta})}{h_1(u_d|\hat{u}_d, \hat{\delta})} du_d \quad (38)$$

where $h_1(\cdot|\hat{u}_d, \hat{\delta})$ is a normal p.d.f. with the following first and second moments

$$\hat{u}_d = \arg \max_{u_d \in \mathbb{R}} [\log g_d(\mathbf{y}_d|u_d, \boldsymbol{\theta}) + \log h(u_d)] \quad \text{and} \quad \hat{\delta}^2 = \left\{ \frac{-\partial^2 [\log g_d(\mathbf{y}_d|u_d, \boldsymbol{\theta}) + \log h(u_d)]}{\partial^2 u_d} \right\} \Big|_{u_d=\hat{u}_d}^{-1}.$$

For multidimensional random area effects, one would need to find a Cholesky decomposition of the variance covariance matrix (cfr. Tuerlinckx et al. (2006) and Bianconcini (2014)), but in case of one dimensional random effect we can just take a square root of $\hat{\delta}^2$. (38) can be approximated by

$$f_d(\mathbf{y}_d|\boldsymbol{\theta}, \varphi) \approx \hat{f}_d(\mathbf{y}_d|\boldsymbol{\theta}, \varphi) = 2^{1/2}\hat{\delta} \sum_{r=1}^m g_d(\mathbf{y}_d|t_{dr}^A, \boldsymbol{\theta}^e)h_d(t_{dr}^A)w_r^A \quad (39)$$

where $t_{dr}^A = \hat{u}_d + \hat{\delta}\sqrt{2}t_r$ and $w_r^A = \exp(t_r^2)w_r$ denote AGQ nodes and weights with t_{dr} and w_r being the classical GQ nodes and weights respectively (Abramowitz and Stegun, 1966). Using (39) we can obtain the approximation of the whole likelihood (36)

$$\hat{l}(\boldsymbol{\theta}) = -\frac{D}{2} \log(2\pi) + \sum_{d=1}^D \log \left\{ 2^{1/2}\hat{\delta} \sum_{r=1}^m \exp \left[\frac{y_{dj}\gamma_{dj}^A - b(\gamma_{dj}^A)}{\varphi} + c(y_{dj}, \varphi) - \frac{t_{dr}^A{}^2}{2} \right] w_r^A \right\}. \quad (40)$$

To estimate the model parameters, we use the score equation based on (40)

$$\hat{\mathcal{S}}(\boldsymbol{\theta}) = \frac{\partial \hat{l}(\boldsymbol{\theta})}{\partial \boldsymbol{\theta}} = \sum_{d=1}^D \frac{\sum_{r=1}^m \mathcal{S}_d(\boldsymbol{\theta}, t_{dr}^A)g(\mathbf{y}_d|\boldsymbol{\theta}, t_{dr}^A)h(t_{dr}^A)w_r^A}{\sum_{r=1}^m g(\mathbf{y}_d|\boldsymbol{\theta}, t_{dr}^A)h(t_{dr}^A)w_r^A} = \sum_{d=1}^D \hat{\mathbb{E}}_{\mathbf{u}|\mathbf{y}} [\mathcal{S}_d(\boldsymbol{\theta}, u_d)]. \quad (41)$$

Further details for the general derivatives under GLVMM are given by Bianconcini (2014). As far as the statistical properties of AGH based estimators are taken into account, Bianconcini (2014) proved their consistency which follows from the relation to the Laplace approximation. Moreover, the estimators are asymptotically normally distributed since they belong to the class of M-estimators (Huber et al., 1964) which are implicitly defined by a function Ψ using an equation $\sum_{d=1}^D \Psi(\mathbf{y}_d, \boldsymbol{\theta}) = 0$. Note that the AGH Ψ function is given in (41). As pointed out by Huber et al. (2004), one needs to verify if the regularity conditions on the log-likelihood function for

the consistency and the asymptotic normality (see R1-R5 from Appendix in the main document) are satisfied for each p.d.f. of y_{dj} . In case of the binomial model these were already checked by Bianconcini (2014) under GLVMM and the proof for GLMM would be identical with a slight change of notation. As far the unit level model is taken into consideration, we can use (40) to obtain the approximate likelihood

$$\hat{l}(\boldsymbol{\theta}) = \sum_{d=1}^D \left\{ -\frac{1}{2} \log \pi + \log \hat{\sigma} + \log \left[\sum_{r=1}^m \exp \left(\sum_{j=1}^{n_d} \log \binom{m_{dj}}{y_{dj}} + \sum_{j=1}^{n_d} y_{dj} (\mathbf{x}_{dj}^t \boldsymbol{\beta} + \delta t_{dk}^A) - \sum_{j=1}^{n_d} m_{dj} \log [1 + \exp \{ \mathbf{x}_{dj}^t \boldsymbol{\beta} + \delta t_{dk}^A \}] - \frac{t_{dk}^{A2}}{2} \right) w_{dk}^A \right] \right\}$$

and the score equations for each parameter

$$\hat{\mathcal{S}}_d(\beta_i; t_{dk}^A) = \sum_{j=1}^{n_d} \left[y_{dj} x_{dji} + \frac{m_{dj} \exp(x_{dji} \beta_i - \delta t_{dk}^A) x_{dji}}{1 + \exp(x_{dji} \beta_i + \delta t_{dk}^A)} \right], \quad i = 1, \dots, p$$

$$\hat{\mathcal{S}}_d(\delta; t_{dk}^A) = \sum_{j=1}^{n_d} \left[y_{dj} t_{dk}^A + \frac{m_{dj} \exp(x_{dji} \beta_i - \delta t_{dk}^A) t_{dk}^A}{1 + \exp(x_{dji} \beta_i + \delta t_{dk}^A)} \right].$$

These equations might be solved using, for example, quasi Newton-Raphson (Bianconcini, 2014) or a different numerical method suitable to solve nonlinear equations. Notice that under this class of models very fast implementation of AGH are available using R statistical package.

Remark 1. *AGQ would not be appropriate for the area-level model due to the lack of the consistency which is shown by the rate of convergence in Bianconcini (2014). To circumvent this problem Jiang (1998a) suggested using the method of simulated moments with an asymptotic order $O(D^{-1})$ which does not depend on n_d . This approach was used by Hobza and Morales (2016).*

D.2 Estimation of EBP

Under the unit-level binomial model, BP $\tilde{\mu}_d^B$ of $\bar{\mu}_d^B$ defined in main document can be obtained using the derivation of Hobza and Morales (2016), that is

$$\tilde{r}_{dl}(\boldsymbol{\theta}) := \mathbb{E}[r_{dl} | \mathbf{y}_d] = \frac{\int_{\mathbb{R}} \frac{\exp(\mathbf{z}_l^t \boldsymbol{\beta} + \delta u_d)}{1 + \exp(\mathbf{z}_l^t \boldsymbol{\beta} + \delta u_d)} g^B(\mathbf{y}_d | u_d, \boldsymbol{\theta}) h(u_d) du_d}{\int_{\mathbb{R}} g^B(\mathbf{y}_d | u_d, \boldsymbol{\theta}) h(u_d) du_d} = \frac{A_{dl}^B(\mathbf{y}_d, \boldsymbol{\theta})}{C_d^B(\mathbf{y}_d, \boldsymbol{\theta})},$$

$$\tilde{\mu}_d^B(\boldsymbol{\theta}) := \mathbb{E}[\mu_d^B | \mathbf{y}_d] = \sum_{l=1}^L N_{dl} \tilde{r}_{dl}(\boldsymbol{\theta}) =: \psi_d^B(\mathbf{d}, \boldsymbol{\theta}) \quad \text{and} \quad \tilde{\mu}_d^B(\boldsymbol{\theta}) = \frac{\tilde{\mu}_d^B}{N_d} \quad (42)$$

$$\tilde{u}_d(\boldsymbol{\theta}) := \mathbb{E}[u_d | \mathbf{y}_d] = \frac{\int_{\mathbb{R}} u_d g^B(\mathbf{y}_d | u_d, \boldsymbol{\theta}) h(u_d) du_d}{\int_{\mathbb{R}} g^B(\mathbf{y}_d | u_d, \boldsymbol{\theta}) h(u_d) du_d} = \frac{A_d^{uB}(\mathbf{y}_d, \boldsymbol{\theta})}{C_d^B(\mathbf{y}_d, \boldsymbol{\theta})},$$

where

$$\begin{aligned}
A_{dl}^B(y_{dj}, \boldsymbol{\theta}) &= \int_{\mathbb{R}} \frac{\exp(\mathbf{z}_l^t \boldsymbol{\beta} + \delta u_d)}{1 + \exp(\mathbf{z}_l^t \boldsymbol{\beta} + \delta u_d)} \exp \left\{ \delta y_d u_d - \sum_{j=1}^{n_d} m_{dj} \log[1 + \exp(\mathbf{x}_{dj}^t \boldsymbol{\beta} + \delta u_d)] \right\} h(u_d) du_d, \\
A_d^{uB} &= \int_{\mathbb{R}} u_d \exp \left\{ \delta y_d u_d - \sum_{j=1}^{n_d} m_{dj} \log[1 + \exp(\mathbf{x}_{dj}^t \boldsymbol{\beta} + \delta u_d)] \right\} h(u_d) du_d, \\
C_d^B(\mathbf{y}_d, \boldsymbol{\theta}) &= \int_{\mathbb{R}} \exp \left\{ \delta y_d u_d - \sum_{j=1}^{n_d} m_{dj} \log[1 + \exp(\mathbf{x}_{dj}^t \boldsymbol{\beta} + \delta u_d)] \right\} h(u_d) du_d.
\end{aligned} \tag{43}$$

The EBP equivalents of \tilde{r}_{dl} , $\tilde{\mu}_d^B$, $\tilde{\mu}_d^B$ and \tilde{u}_d are $\hat{p}_{dl}^c = \tilde{p}_{dl}^c(\hat{\boldsymbol{\theta}})$, $\hat{\mu}_d^B = \tilde{\mu}_d^B(\hat{\boldsymbol{\theta}})$, $\hat{\mu}_d^B = \tilde{\mu}_d^B(\hat{\boldsymbol{\theta}})$ and $\hat{u}_d = \tilde{u}_d(\hat{\boldsymbol{\theta}})$ where $\hat{\boldsymbol{\theta}}$ is a consistent estimator of $\boldsymbol{\theta}$. They can be calculated using a Monte Carlo simulation, as described in detail by Hobza and Morales (2016).

D.3 Consistency of SCI

?? Proof of consistency of SCI under the unit-level logit model proceeds along the same lines as in case of the area-level model, i.e., we start with the expansion of $G_d(w)$ as in Section C.3. In the second part, specific to the unit-unit level logit model, we would use the expansions provided in Hobza and Morales (2016), p. 668-671 and their appendix.

D.4 Finite sample performance

A detailed setting of the simulation under the unit-level model is described in the main document. In what follows we shall present the exact algorithm to obtain SCI and iCI and additional numerical results. Employing the simulation steps of Hobza and Morales (2016), p.671, we provide below a shortened version of the algorithm to obtain SCI bands under unit-level binomial model.

1. Follow the steps of the parametric bootstrap procedure from Hobza and Morales (2016), p.671.
2. Calculate $AD_{B,d}^{(b_1)} = \left| \hat{\mu}_d^{*(b_1)} - \bar{\mu}_d^{*(b_1)} \right|$.
3. Compute the estimated statistic S and the critical value $q_{1-\alpha}^*$

$$S_{B,B}^{(b_1)} = \max_{d=1,\dots,D} \frac{AD_{B,d}^{*(b_1)}}{\hat{\sigma}^*} \quad \text{and} \quad q_{B,S_B}(1-\alpha) = Q_{1-\alpha}(\mathbf{S}_{B,B}) \quad \text{where} \quad \mathbf{S}_{B,B} = (S_{B,B}^{(1)}, \dots, S_{B,B}^{(B_1)})^t,$$

the estimated statistic R and the critical value $q_{R_B}(1 - \alpha)$

$$R_{B,B}^{(b_1)} = \max_{d=1,\dots,D} AD_{B,d}^{*(b_1)} \quad \text{and} \quad q_{B,R_B}(1-\alpha) = Q_{1-\alpha}(\mathbf{R}_{B,B}) \quad \text{where} \quad \mathbf{R}_{B,B} = (R_{B,B}^{(1)}, \dots, R_{B,B}^{(B_1)})^t,$$

as well as the variance of θ

$$\widehat{\text{var}}(\hat{\theta}) = \frac{1}{B_1} \sum_{b_1=1}^{B_1} (\hat{\theta}^{*(b_1)} - \bar{\theta})(\hat{\theta}^{*(b_1)} - \bar{\theta})^t$$

where $\bar{\theta} = \frac{1}{B_1} \sum_{b_1=1}^{B_1} \hat{\theta}^{*(b_1)}$.

| D | $\hat{\beta}_0$ | $\hat{\beta}_1$ | $\hat{\beta}_2$ | $\hat{\beta}_3$ | $\hat{\beta}_4$ | $\hat{\delta}$ |
|----|------------------|------------------|------------------|------------------|------------------|------------------|
| 26 | 0.0027 (0.0451) | -0.0050 (0.0682) | 0.0058 (0.2990) | -0.0083 (0.1017) | -0.0485 (0.6725) | -0.0572 (0.1903) |
| 52 | -0.0042 (0.0360) | -0.0013 (0.0537) | 0.0176 (0.2415) | 0.0088 (0.0726) | 0.0118 (0.4895) | -0.0022 (0.1367) |
| 78 | -0.0027 (0.0263) | 0.0037 (0.0418) | -0.0046 (0.1773) | 0.0043 (0.0645) | -0.0081 (0.4163) | -0.0170 (0.1035) |

Table 6: RBIAS and RRMSE (in parenthesis) for AGQ estimators.

Table 6 outlines RBIAS and RRMSE of θ . Similarly to the area-level Poisson model, the quality of estimates improves with a growing sample size. On the other hand, a very good performance of EBP of p_d is shown in Table 7. When it comes to relative bias and relative root MSE of EBP for p_d in Figure 14, their behaviour is similar to their equivalents under the area-level model, nevertheless with the higher magnitude.

| D | d | $B_d(E_d)$ | D | d | $B_d(E_d)$ | D | d | $B_d(E_d)$ |
|------|----|------------------|------|----|------------------|------|----|------------------|
| 26 | 6 | -0.0008 (0.0002) | 52 | 11 | -0.0007 (0.0002) | 78 | 16 | -0.0013 (0.0002) |
| | 11 | -0.0004 (0.0003) | | 21 | -0.0001 (0.0003) | | 32 | -0.0003 (0.0003) |
| | 16 | -0.0002 (0.0005) | | 32 | 0.0005 (0.0005) | | 47 | 0.0003 (0.0005) |
| | 21 | 0.0002 (0.0008) | | 42 | 0.0015 (0.0008) | | 63 | 0.0013 (0.0008) |
| B(E) | | 0.0007 (0.0005) | B(E) | | 0.0010 (0.0005) | B(E) | | 0.0012 (0.0005) |

Table 7: B_d , E_d and their averages B and E for the estimators of p_d under unit-level binomial model.

The estimates of MSE behave similarly as in Hobza and Morales (2016) as it can be seen in Figure 15.

Figure 16 displays iCI and SCIs under the unit-level model for a randomly selected simulation. Red dots represents true area proportions which are outside of their iCI. We can draw the same conclusions as in case of the area-level model. Finally, Figure 17 presents results of the multiple testing procedure. Already for $D=26$, the power of the test attains te nominal level of $\alpha = 0.05$.

References

- Abramowitz, M. and Stegun, I. (1966). Handbook of mathematical functions. *Am. J. Phys*, 34(2):177–177.
- Bianconcini, S. (2014). Asymptotic properties of adaptive maximum likelihood estimators in latent variable models. *Bernoulli*, 20(3):1507–1531.

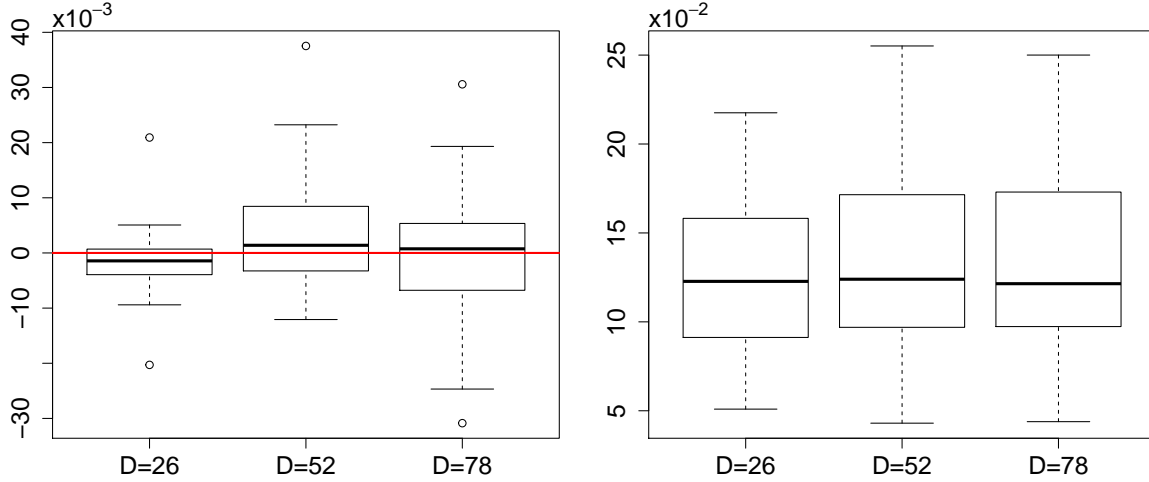


Figure 14: Box plots with (left) RBIAIS and (right) RRMSE for \hat{p}_d under the unit-level model.

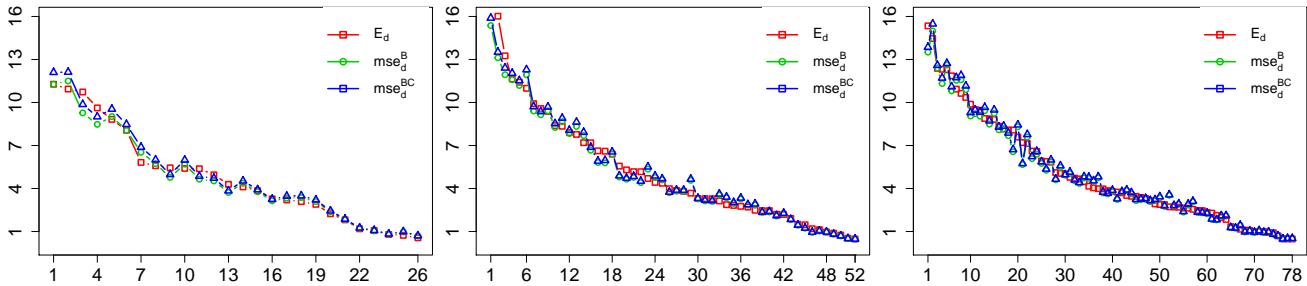


Figure 15: MSE estimators ($\times 10^4$): (left) $D = 26$, (centre) $D = 52$ and (right) $D = 78$ under area-level Poisson model.

Boubeta, M., Lombardía, M. J., and Morales, D. (2016). Empirical best prediction under area-level poisson mixed models. *Test*, 25(3):548–569.

Breslow, N. E. and Clayton, D. G. (1993). Approximate inference in generalized linear mixed models. *J. Am. Stat. Assoc.*, 88(421):9–25.

Chatterjee, S., Lahiri, P., and Li, H. (2008). Parametric bootstrap approximation to the distribution of EBLUP and related prediction intervals in linear mixed models. *Ann. Statist.*, 36(3):1221–1245.

De Bruijn, N. G. (1981). *Asymptotic methods in analysis*. Courier Corporation.

Demidenko, E. (2013). *Mixed models: theory and applications with R*. John Wiley & Sons.

DiCiccio, T. J. and Efron, B. (1996). Bootstrap confidence intervals. *Statist. Sci.*, 11(3):189–228.

Fisher, R. A. and Tippett, L. H. C. (1928). Limiting forms of the frequency distribution of the

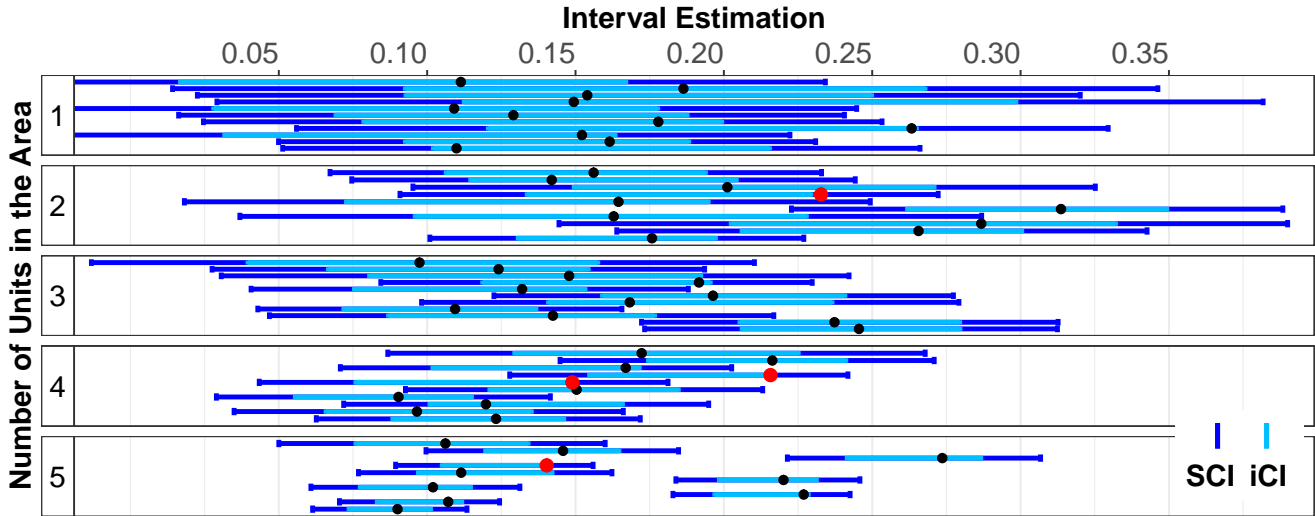


Figure 16: iCI and bootstrap SCI for proportions, $D = 52$. Red dots denote true estimates outside iCI.

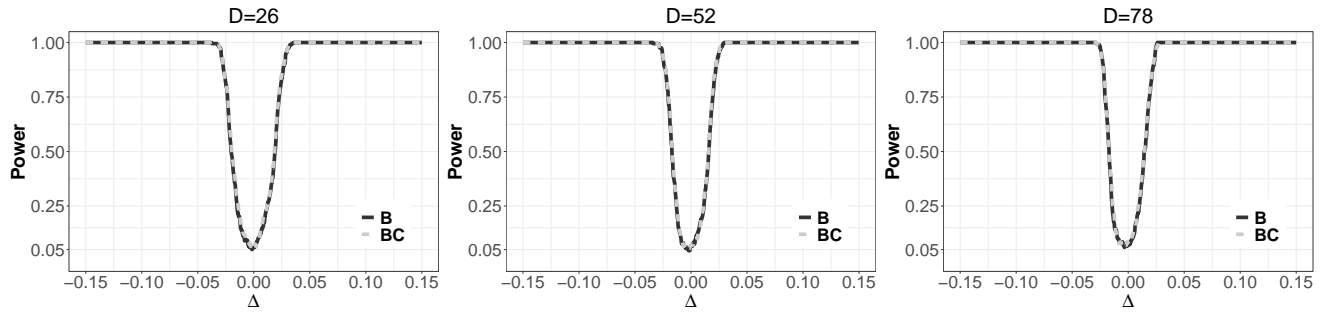


Figure 17: Simulated power for testing $H_0 : \bar{\mu} = \mathbf{h}$ versus $H_1 : \bar{\mu} = \mathbf{h} + \mathbf{1}_D \Delta$; (left) $D = 26$, (center) $D = 52$, (right) $D = 78$.

largest or smallest member of a sample. *Proceedings of the Cambridge Philosophical Society*, 24:180.

Ganesh, N. (2009). Simultaneous credible intervals for small area estimation problems. *J. Multivariate Anal.*, 100(8):1610–1621.

Hall, P. and Maiti, T. (2006a). Nonparametric estimation of mean-squared prediction error in nested-error regression models. *Ann. Statist.*, 34(4):1733–1750.

Hall, P. and Maiti, T. (2006b). On parametric bootstrap methods for small area prediction. *J. R. Statist. Soc. B*, 68(2):221–238.

Hidiroglou, M. A. and You, Y. (2016). Comparison of unit level and area level small area estimators. *Surv. Methodol.*, 42(42):41–61.

- Hobza, T. and Morales, D. (2016). Empirical best prediction under unit-level logit mixed models. *J. Off. Stat.*, 32(3):661–692.
- Hothorn, T., Bretz, F., and Westfall, P. (2008). Simultaneous inference in general parametric models. *Biom. J.*, 50(3):346–363.
- Huber, P., Ronchetti, E., and Victoria-Feser, M.-P. (2004). Estimation of generalized linear latent variable models. *J. R. Statist. Soc. B*, 66(4):893–908.
- Huber, P. J. et al. (1964). Robust estimation of a location parameter. *Ann. Math. Statist.*, 35(1):73–101.
- Jiang, J. (1998a). Asymptotic properties of the empirical blup and blue in mixed linear models. *Stat. Sin.*, pages 861–885.
- Jiang, J. (1998b). Consistent estimators in generalized linear mixed models. *J. Am. Statist. Ass.*, 93(442):720–729.
- Jiang, J. (2003). Empirical best prediction for small-area inference based on generalized linear mixed models. *J. Stat. Plan. Inference*, 111(1-2):117–127.
- Jiang, J. (2007). *Linear and generalized linear mixed models and their applications*. Springer Science & Business Media.
- Jiang, J. and Lahiri, P. (2001). Empirical best prediction for small area inference with binary data. *Ann. Inst. Stat. Math.*, 53(2):217–243.
- Joe, H. (2008). Accuracy of laplace approximation for discrete response mixed models. *Comput. Statist. Data Anal.*, 52(12):5066–5074.
- Kramlinger, P., Krivobokova, T., and Sperlich, S. (2018). Marginal and conditional multiple inference in linear mixed models. *arXiv:1812.09250*.
- Krivobokova, T., Kneib, T., and Claeskens, G. (2010). Simultaneous confidence bands for penalized spline estimators. *J. Am. Statist. Ass.*, 105(490):852–863.
- Lawless, J. F. (1987). Negative binomial and mixed poisson regression. *Can. J. Stat.*, 15(3):209–225.
- Leadbetter, M. R., Lindgren, G., and Rootzén, H. (2012). *Extremes and related properties of random sequences and processes*. Springer Science & Business Media.
- López-Vizcaíno, E., Lombardía, M. J., and Morales, D. (2015). Small area estimation of labour force indicators under a multinomial model with correlated time and area effects. *J. R. Statist. Soc. A*, 178(3):535–565.

- Maringwa, J. T., Geys, H., Shkedy, Z., Faes, C., Molenberghs, G., Aerts, M., Ammel, K. V., Teisman, A., and Bijnen, L. (2008). Application of semiparametric mixed models and simultaneous confidence bands in a cardiovascular safety experiment with longitudinal data. *J. Biopharm. Stat.*, 18(6):1043–1062.
- Namazi-Rad, M.-R. and Steel, D. (2015). What level of statistical model should we use in small area estimation? *Aust N Z J Stat*, 57(2):275–298.
- Naylor, J. C. and Smith, A. F. (1982). Applications of a method for the efficient computation of posterior distributions. *J. R. Statist. Soc. C*, 31(3):214–225.
- Pinheiro, J. C. and Bates, D. M. (1995). Approximations to the log-likelihood function in the nonlinear mixed-effects model. *J. Comput. Graph. Stat.*, 4(1):12–35.
- Pratesi, M. (2016). *Analysis of poverty data by small area estimation*. John Wiley & Sons.
- Rabe-Hesketh, S., Skrondal, A., and Pickles, A. (2005). Maximum likelihood estimation of limited and discrete dependent variable models with nested random effects. *J. Econom.*, 128(2):301–323.
- Rao, J. N. and Molina, I. (2015). *Small area estimation*. John Wiley & Sons.
- Reluga, K., José Lombardía, M., and Sperlich, S. A. (2019). Simultaneous Prediction Intervals for Small Area Parameter. *arXiv:1903.02774*.
- Ritz, C., Pilmann Laursen, R., and Trab Damsgaard, C. (2017). Simultaneous inference for multilevel linear mixed models—with an application to a large-scale school meal study. *J. R. Statist. Soc. C*, 66(2):295–311.
- Ruppert, D., Wand, M. P., and Carroll, R. J. (2003). *Semiparametric regression*. CUP.
- Schervish, M. J. (2012). *Theory of statistics*. Springer Science & Business Media.
- Stiratelli, R., Laird, N., and Ware, J. H. (1984). Random-effects models for serial observations with binary response. *Biometrics*, 40(4):961–971.
- Tuerlinckx, F., Rijmen, F., Verbeke, G., and De Boeck, P. (2006). Statistical inference in generalized linear mixed models: A review. *Br. J. Math. Stat. Psychol.*, 59(2):225–255.
- Wagler, A. E. (2014). Confidence intervals for assessing heterogeneity in generalized linear mixed models. *J. Educ. Behav. Stat.*, 39(3):167–179.
- Weyl, H. (1939). On the volume of tubes. *Am. J. Math.*, 61(2):461–472.